Since January 2020 Elsevier has created a COVID-19 resource centre with free information in English and Mandarin on the novel coronavirus COVID-19. The COVID-19 resource centre is hosted on Elsevier Connect, the company's public news and information website.

Results in Physics 34 (2022) 105224

Contents lists available at ScienceDirect

Results in Physics

journal homepage: www.elsevier.com/locate/rinp

The influence of mask use on the spread of COVID-19 during pandemic in New York City

Xia Ma [a,b,c], Xiao-Feng Luo [b], Li Li [d], Yong Li [e], Gui-Quan Sun [a,b,f,*]

[a] School of Big Data, North University of China, Taiyuan, 030051, China
[b] Department of Mathematics, North University of China, Taiyuan, 030051, China
[c] Department of Science, Taiyuan Institute of Technology, Taiyuan, 030008, China
[d] School of Computer and Information Technology, Shanxi University, Taiyuan, 030006, China
[e] School of Information and Mathematics, Yangtze University, Jingzhou, 434023, China
[f] Complex Systems Research Center, Shanxi University, Taiyuan, 030006, China

ARTICLE INFO

Keywords:
COVID-19
Face mask
Basic reproduction number
Parameter estimation
Markov chain
Sensitivity analysis

ABSTRACT

In New York City, the situation of COVID-19 is so serious that it has caused hundreds of thousands of people to be infected due to its strong infectivity. The desired effect of wearing masks by the public is not ideal, though increasingly recommended by the WHO. In order to reveal the potential effect of mask use, we posed a dynamical model with the effective coverage of wearing face masks to assess the impact of mask use on the COVID-19 transmission. We obtained the basic reproduction number R_0 which determined the global dynamics. According to the implement of policies in New York City, we divided the transmission of COVID-19 in three stages. Based on mathematical model and data, we obtain the mean value $R_0 = 1.822$ in the first stage of New York City, while $R_0 = 0.6483$ in the second stage due to that the US Centers for Disease Control and Prevention (CDC) recommended the public wear masks on April 3, 2020, $R_0 = 1.024$ in the third stage after reopening. It was found that if the effective coverage rate of mask use α exceed a certain value $\alpha_c = 0.182$, COVID-19 can be well controlled in the second stage of New York City. Additionally, when the effective coverage of masks reaches a certain level $\alpha = 0.5$, the benefits are not obvious with the increased coverage rate compared to the cost of medical resources. Moreover, if the effective coverage of mask use in public reaches 20% in the first stage, then the cumulative confirmed cases will be reduced about 50% by 03 April, 2020. Our results demonstrated a new insight on the effect of mask use in controlling the transmission of COVID-19.

Introduction

Coronaviruses can cause disease pandemic, which are single-stranded, positive RNA viruses belonging to the family of Coronaviridae [1]. They can affect mammals, causing commonly mild infectious disease, occasionally leading to severe outbreaks clusters, such as the SARS virus, and the MERS virus [2]. COVID-19 is an infectious disease caused by a newly discovered coronavirus which is distinct from them. The COVID-19 virus can be transmitted by three main routes including direct transmission, contact transmission and aerosol [3]. Due to the absence of specific COVID-19 therapeutic and effective vaccine, making it very difficult to control the transmission [4]. To prevent the infection and further transmission of COVID-19, a range of nonpharmaceutical interventions has been used to control the epidemic [5]. For the moment, the spread of the epidemic was basically controlled and life quickly returned to normal in China through the efforts of the whole country. However, the endemic is still very grim of abroad, such as USA, Europe, Brazil, India.

The United States is one of the worst affected countries by COVID-19 in the world. The New York City (NYC), as the most prosperous city of the United States, the population density is very high and the communication between people is relatively frequent. Therefore, the New York City metropolitan area quickly became the hardest-hit region of the COVID-19 pandemic following by the first confirmed cases on March 2, 2020 [6]. In the early stage of the COVID-19 epidemic, mask use in public has been controversial, few people in the public wear masks in the liberal and democratic society of the United States, and people who wear masks are regarded as disseminators of the virus. Some people are afraid of wearing masks for fear of opposition. In addition, due to the shortage of medical resources, especially in the supply of masks, there are not enough masks for ordinary people, the percentage of people wearing masks was very low. Hence, the

* Corresponding author at: Department of Mathematics, North University of China, Taiyuan, 030051, China.
E-mail address: gquansun@126.com (G.-Q. Sun).

https://doi.org/10.1016/j.rinp.2022.105224
Received 1 February 2021; Received in revised form 11 January 2022; Accepted 12 January 2022
Available online 22 January 2022

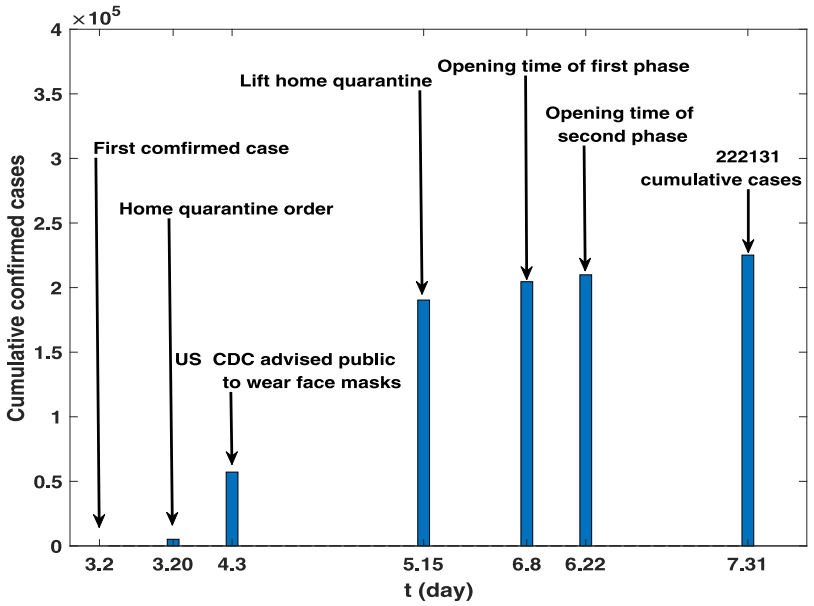

Fig. 1. Time series diagram of COVID-19 in New York City [6,8,9].

confirmed cases of COVID-19 in New York City increased rapidly, and then more than 60,000 cases have been confirmed in just one month followed by the first confirmed case [6].

Although on April 3, 2020, the US Centers for Disease Control and Prevention (CDC) recommended the public wear cloth masks [7], the proportion of people wearing masks in public space is still relatively small in New York City. As a result, the accumulated confirmed cases of COVID-19 quickly swelled to hundreds of thousands in few months. With the relieving of lockdown in New York City, the first phase of the restart is on June 8, and the second phase is on June 22 [8]. People gradually returned to normal work, then the contacts between people are relatively frequent. The time series diagram of COVID-19 and recent opening and closing policy decisions in New York City are shown in Fig. 1. If people do not take personal protection, this will increase the risk of transmission. Instead, the public use of masks is very common in Asian countries, which has rich experience in dealing with COVID-19 epidemic [7].

The protective effect of wearing masks has been controversial, despite experimental result demonstrates face masks can effectively prevent the spread of droplets and aerosols [10]. Some researches revealed that face masks could be a useful intervention strategy. If N95 respirators have 20% effect on reducing the infectivity, to reduce the number of influenza A cases by 20%, there are 10% people would have to wear them [11]. Masks have also been used as a way to prevent the transmission by asymptomatic or clinically undetected carriers, who may be a major driver of the spread of COVID-19 [12,13]. The widespread use of masks is a striking feature of Taiwan's relative success in responding to COVID-19 [14]. Case control data for 2003 SARS epidemic showed that use of masks in public places has a strong protective value for community members [15,16]. Due to the shortage of medical resources, especially in the supply of masks, masks are mainly provided to some doctors and patients, not to ordinary people in some country. Therefore, people's behavior change during infectious disease outbreaks have significant influence in controlling the disease spread, then investigating the correlation between the coverage of wearing masks and the infection dynamics in NYC becomes very important during the COVID-19 outbreak. There are many researches about the transmission of COVID-19 epidemic in NYC. Harrichandra et al. [17] indicated that appropriate outdoor airflow rates, the use of face masks and social distance have the potential to reduce the risk of COVID-19 transmission in NYC nail salons. Alagoz et al. [18] characterized timing of implementing and relaxing social distancing intervention has crucial effects on the number of COVID-19 cases in NYC. Wilder et al. [19] adopted an individual-level model for COVID-19 transmission to explain the location-dependent distributions of age, family structure, and comorbidities in NYC.

Dynamical modeling can better help understand the transmission mechanism of diseases spread as well as COVID-19, which can dynamically predict the future transmission trend according to the current information. Steffen et al. used a dynamical model to characterize the effect of face masks about the transmission of COVID-19 in New York state before April 3, 2020, and revealed use of face masks by the general public is potentially of high value in curtailing community transmission and the burden of the pandemic [7]. Tang et al. devised a SEIR model on the estimation of the transmission risk of COVID-19 and showed the effectiveness of control strategy by intensive contact tracing followed by quarantine and isolation [20]. Sun et al. presented a dynamical model to show the propagation of COVID-19 in Wuhan and the effects of lockdown and medical resources [21]. To our knowledge there are few studies using dynamic model to discuss the effects of mask use about the transmission of COVID-19 in NYC.

In order to investigate the transmission mechanism of COVID-19 and the influence of the coverage of mask use in NYC, we proposed a deterministic differential dynamical model and explore the corresponding global dynamics motivated by the above ideas. Moreover, we estimate the key parameter values about the coverage of mask use and the transmission rate by extensive Markov-chain Monte-Carlo simulations. Next, sensitivity analysis was carried out to identify parameters affecting the disease transmission most. We explore the impact between the coverage of mask use by public and the disease transmission. Finally, some conclusion and discussion are given.

Dynamical modeling of COVID-19 transmission in New York City

Masks use is useful for both preventing illness in healthy people and asymptomatic transmission [7]. In order to investigate the transmission mechanism and the influence of the coverage about mask use of COVID-19 in NYC, we pose a deterministic differential dynamical model with the coverage rate of mask use. We divide the total population as six groups: Susceptible (S), Exposed (E), Asymptomatic infected (A), Symptomatic infected (I), Diagnosed and treated (Q) and Removed (R)(Here, removed group includes recovered and death populations).

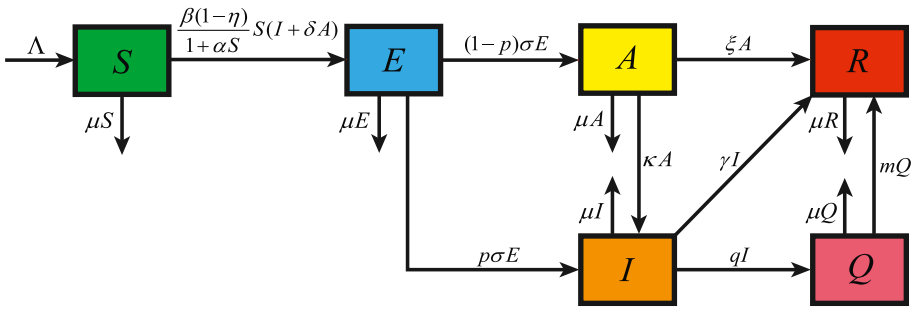

Fig. 2. Transmission diagram of COVID-19 in New York city.

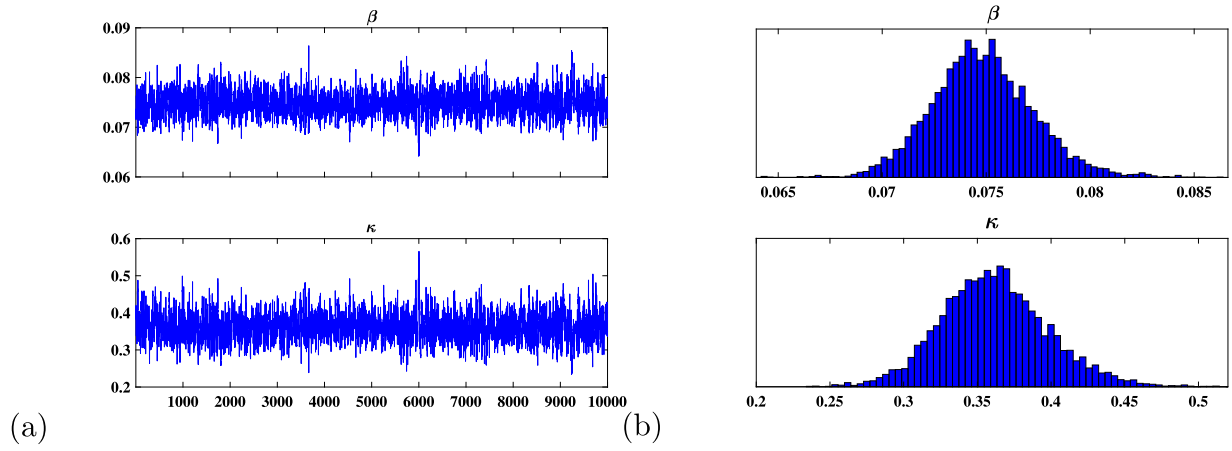

Fig. 3. (a) Simulation results for parameter β and κ of Markov chain with 10 000 sample realizations. (b) The histogram of parameter β and κ in the first stage.

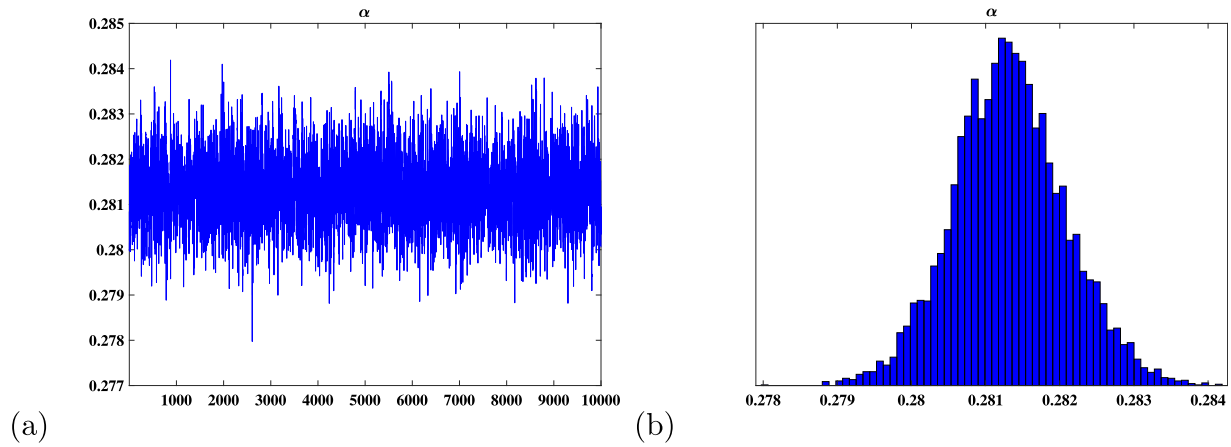

Fig. 4. (a) Simulation results for parameter α of Markov chain with 10 000 sample realizations. (b) The histogram of parameter α in the second stage.

To better investigate the COVID-19 model, we suppose that the asymptomatic infected (A) and symptomatic infected (I) populations all have ability to infect the susceptible populations (S), but the exposed (E) cannot. We also assume the people diagnosed and treated in hospital (Q) are not exposed to the general population and do not contribute to infection rates. The transformation block diagram is in Fig. 2 and the parameters are described in Table 1. Consequently, the differential SEAIQR model is as follows:

$$\begin{cases} \frac{dS(t)}{dt} = \Lambda - \frac{\beta(1-\eta)}{1+\alpha S}S(I+\delta A) - \mu S, \\ \frac{dE(t)}{dt} = \frac{\beta(1-\eta)}{1+\alpha S}S(I+\delta A) - (\mu+\sigma)E, \\ \frac{dA(t)}{dt} = (1-p)\sigma E - (\mu+\kappa+\xi)A, \\ \frac{dI(t)}{dt} = p\sigma E + \kappa A - (\mu+q+\gamma)I, \\ \frac{dQ(t)}{dt} = qI - (m+\mu)Q, \\ \frac{dR(t)}{dt} = \xi A + \gamma I + mQ - \mu R. \end{cases} \tag{1}$$

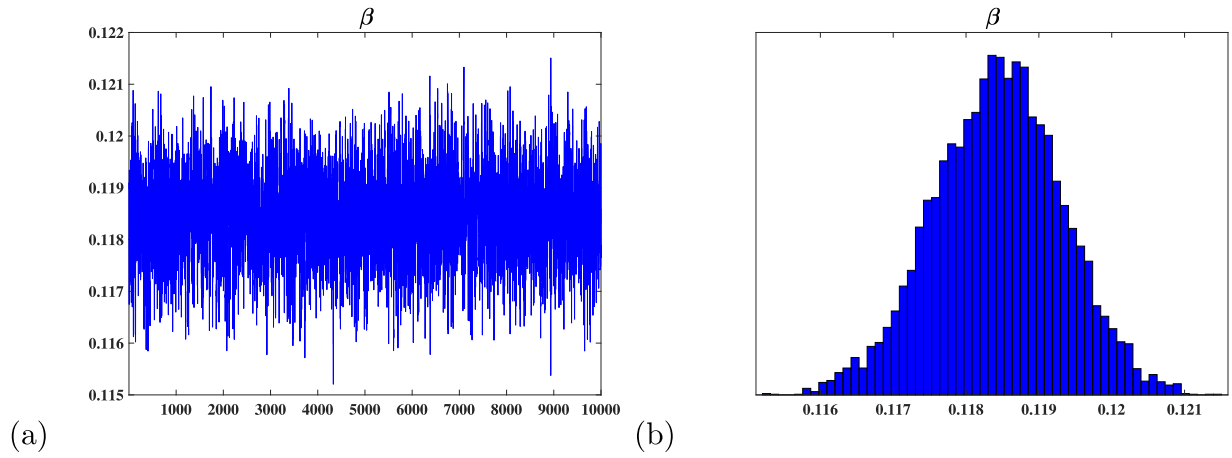

Fig. 5. (a) Simulation results for parameter β of Markov chain with 10 000 sample realizations in the third stage. (b) The histogram of parameter β in the third stage.

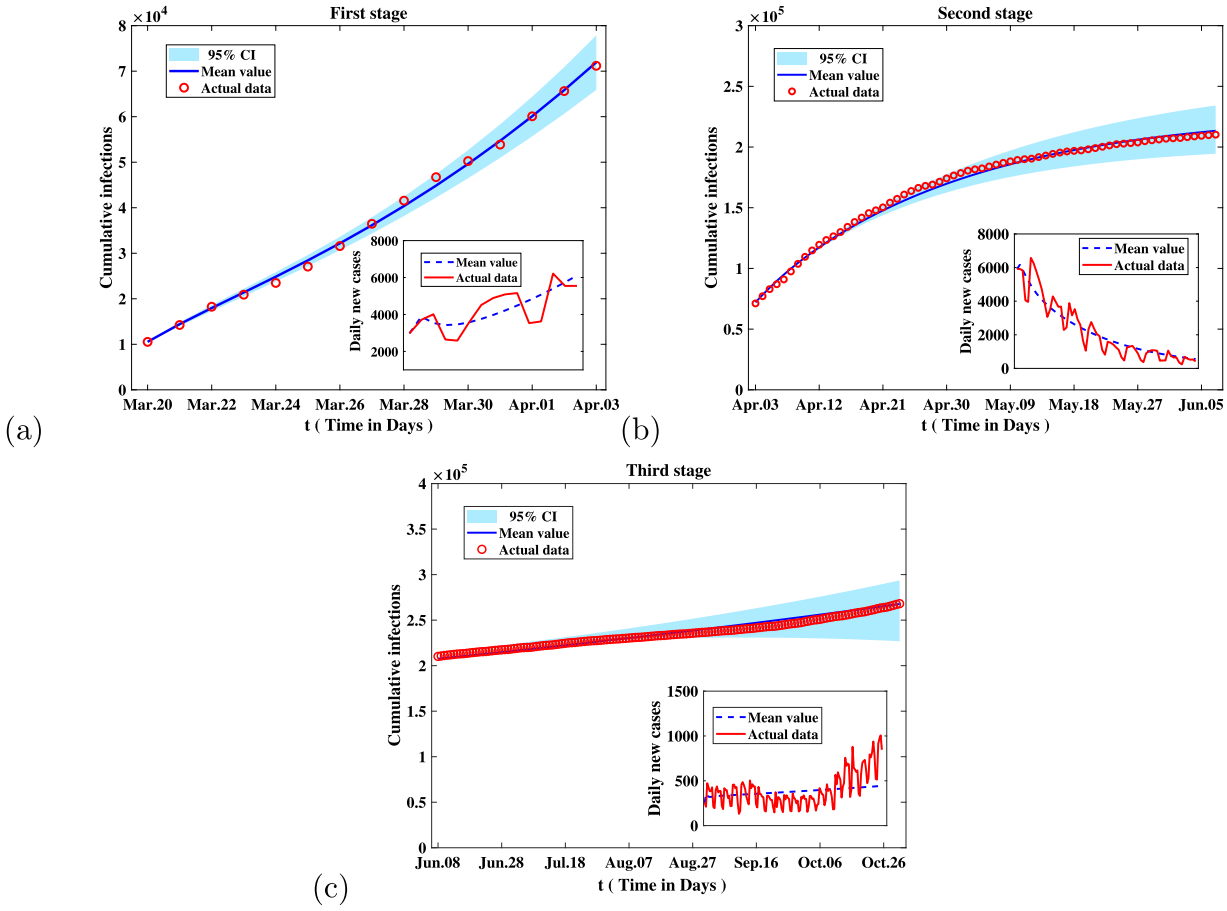

Fig. 6. Fitting results of cumulative infected cases and daily new infected cases from March 20 to October 31, 2020. The red circles are the number of cumulative infected cases and the blue solid curves represents the estimated cumulative infected cases with the shadow areas as the corresponding 95% confidence band. The red solid curve expresses the number of new daily confirmed cases, the blue dotted curve represents the predicted daily new cases. (a) Fitting results of cumulative infected cases and daily new infected cases in New York City from March 20 to April 03, 2020; (b) Fitting results of cumulative infected cases and daily new infected cases from April 03 to June 07, 2020. (c) Fitting results of cumulative infected cases and daily new infected cases from June 08 to October 31, 2020. (For interpretation of the references to color in this figure legend, the reader is referred to the web version of this article.)

In the model, parameter α is the effective coverage rate of mask use by the public, which is equal to the coverage rate of mask use products the efficacy of mask. When parameter $\alpha = 0$, model is equivalent to the bilinear incidence, such case can account for the intense competition for medical resources due to the limited medical resources in the early stage of the epidemic, which means there is no masks supplied to the ordinary people. Since the proportion of susceptible individuals is relative large, $\alpha = 1$ means all susceptible individuals wear masks under the condition that the supply of masks is very sufficient and masks provide 100% protection, $\frac{\beta(1-\eta)}{1+\alpha S}$ is approximately equal to zero as S is sufficiently large, which can account for all susceptible wear masks, and there is small probability to be infected, where $0 < \alpha < 1$ means partial susceptible individuals wear masks.

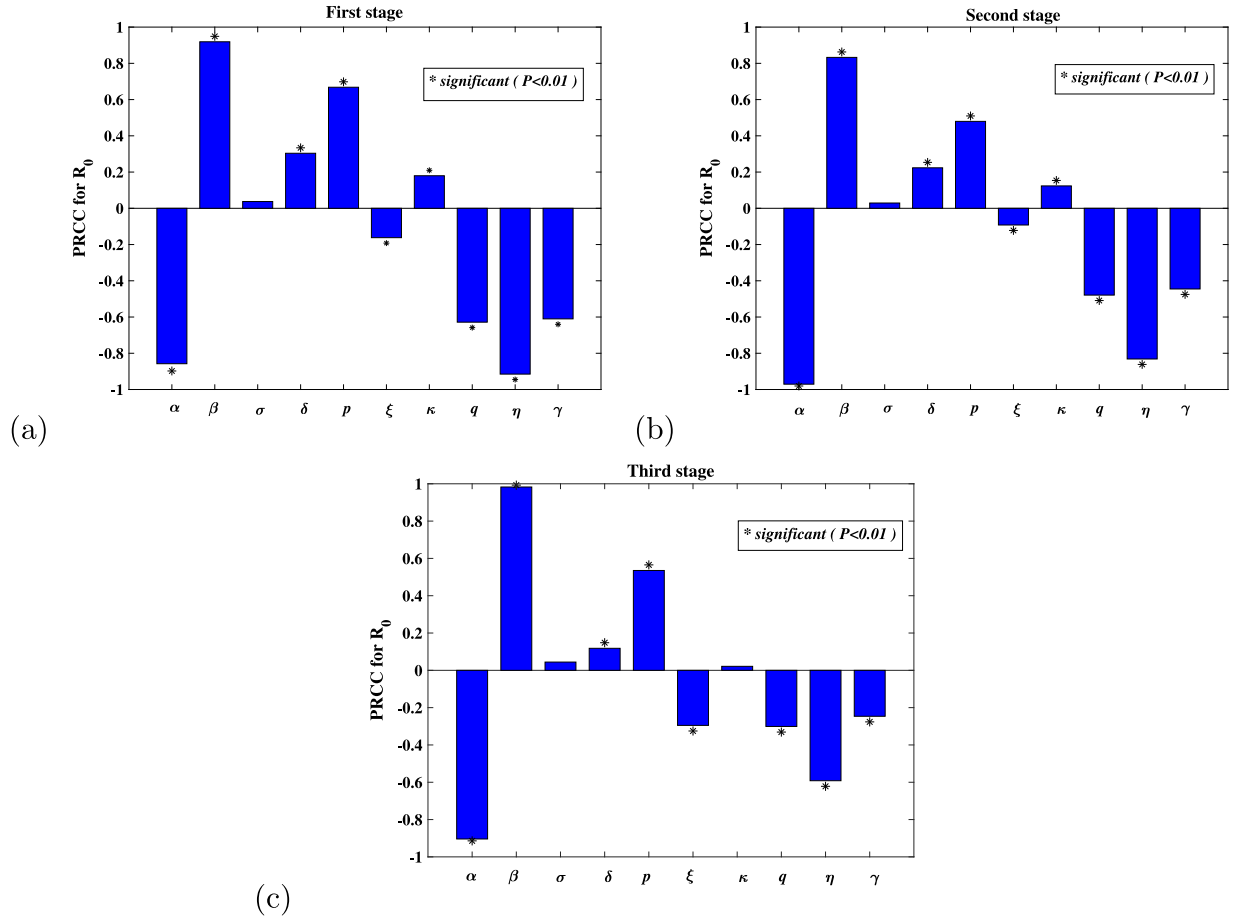

Fig. 7. (a) PRCC value of R_0 with $\alpha = 0.1$ in the first stage; (b) PRCC value of R_0 with $\alpha = 0.2813$ in the second stage; (c) PRCC value of R_0 with $\beta = 0.1184$ in the third stage.

Table 1
Definitions of frequently used variables and parameters of model (1).

Variables	Description
$S(t)$	The susceptible individuals at time t
$E(t)$	The exposed individuals at time t
$A(t)$	The asymptomatic infected individuals at time t
$I(t)$	The symptomatic infected individuals at time t
$Q(t)$	The diagnosed and treated individuals via the medical care at time t
$R(t)$	The removed individuals at time t
β	The transmission rate of infected individuals
η	The rate of keeping social distance
α	The effective coverage rate of wearing masks by the public
μ	Natural death rate
δ	Relative transmission probability of $A(t)$ compared with $I(t)$
σ	Progression rate of exposed individuals to infectives
p	Progression rate from exposed individuals to symptomatic infectives
κ	Progression rate from $A(t)$ to $I(t)$
ξ	Recovery rate of asymptomatic infected individuals
q	Progression rate from $I(t)$ to $Q(t)$
γ	Recovery rate of symptomatic infected individuals
m	Recovery rate of hospitalized individuals

It is easy to show that all solutions of system (1) with positive initial conditions are defined on $[0, +\infty)$ and remain positive for all $t > 0$. We can verify the domain

$$\Omega = \left\{ (S, E, A, I, Q, R) \in \mathbb{R}^6_+ \mid S + E + A + I + Q + R \le \frac{\Lambda}{\mu} \right\}.$$

is a compact and positively invariant set of model (1), which implies that $S(t)$, $E(t)$, $A(t)$, $I(t)$, $Q(t)$,$R(t)$ are bounded in the invariant set Ω.

Basic reproduction number and global dynamics

Basic reproduction number

Model (1) always has a disease-free equilibrium $P^0 = (S^0, 0, 0, 0, 0, 0)$ for any parameter values, where $S^0 = \frac{\Lambda}{\mu}$. According to the approach of next generation matrix [22,23], the associated next generation matrices are given by

$$F = \begin{pmatrix} 0 & \frac{\beta(1-\eta)\delta S^0}{1+\alpha S^0} & \frac{\beta(1-\eta) S^0}{1+\alpha S^0} \\ 0 & 0 & 0 \\ 0 & 0 & 0 \end{pmatrix},$$

$$V = \begin{pmatrix} \mu+\sigma & 0 & 0 \\ -(1-p)\sigma & \mu+\kappa+\xi & 0 \\ -p\sigma & -\kappa & \mu+q+\gamma \end{pmatrix}.$$

The inverse of V equals to

$$V^{-1} = \begin{pmatrix} \frac{1}{\mu+\sigma} & 0 & 0 \\ \frac{(1-p)\sigma}{(\mu+\sigma)(\mu+\kappa+\xi)} & \frac{1}{\mu+\kappa+\xi} & 0 \\ \frac{p\sigma(\mu+\kappa+\xi)+\kappa(1-p)\sigma}{(\mu+\sigma)(\mu+\kappa+\xi)(\mu+q+\gamma)} & \frac{\kappa}{(\mu+\kappa+\xi)(\mu+q+\gamma)} & \frac{1}{\mu+q+\gamma} \end{pmatrix}.$$

The basic reproduction number R_0 of model (1) is defined by the spectral radius of FV^{-1}, namely,

$$R_0 = \frac{\beta(1-\eta)S^0}{1+\alpha S^0}\left[\frac{(1-p)\sigma\delta}{(\mu+\sigma)(\mu+\xi+\kappa)} + \frac{(1-p)\sigma\kappa}{(\mu+\sigma)(\mu+\kappa+\xi)(\mu+q+\gamma)} + \frac{p\sigma}{(\mu+\sigma)(\mu+q+\gamma)}\right].$$

Strength number

In the field of epidemiology, the basic reproduction number has always been an important threshold parameter for measuring whether a disease can spread in a population. As the approach in the above, we can seek out two matrices F and V, hence $\det(FV^{-1} - \lambda I) = 0$ can be derived the basic reproduction number. The matrix F can be received by deducing the nonlinear part of the newly infected items. Here,

$$\frac{\partial}{\partial I}\Big(\frac{\beta(1-\eta)}{1+\alpha S}S(I+\delta A)\Big) = \frac{\beta(1-\eta)S}{1+\alpha S},$$
$$\frac{\partial}{\partial A}\Big(\frac{\beta(1-\eta)}{1+\alpha S}S(I+\delta A)\Big) = \frac{\beta(1-\eta)\delta S}{1+\alpha S}.$$

$$\frac{\partial^2}{\partial I^2}\Big(\frac{\beta(1-\eta)}{1+\alpha S}S(I+\delta A)\Big) = \frac{\partial}{\partial I}\Big(\frac{\beta(1-\eta)S}{1+\alpha S}\Big) = 0,$$
$$\frac{\partial^2}{\partial A^2}\Big(\frac{\beta(1-\eta)}{1+\alpha S}S(I+\delta A)\Big) = \frac{\partial}{\partial I}\Big(\frac{\beta(1-\eta)\delta S}{1+\alpha S}\Big) = 0.$$

Therefore, the following holds at the disease-free equilibrium

$$F_A = \begin{pmatrix} 0 & 0 & 0 \\ 0 & 0 & 0 \\ 0 & 0 & 0 \end{pmatrix}.$$

Furthermore, $\det(F_A V^{-1} - \lambda I) = 0$ can contribute to $A_0 = 0$, which means that the transmission will not exist a renewal process, and hence there will have a single magnitude and extinct. $A_0 > 0$ suggests that there exists enough strength that will result in renewal process, therefore the transmission will have more than one wave [24].

Global dynamic of disease-free equilibrium

Theorem 1. *When $R_0 < 1$, the disease-free equilibrium $P^0 = (S^0, 0, 0, 0, 0, 0)$ of model (1) is globally asymptotically stable.*

Proof. The linearized matrix of model (1) at the disease-free equilibrium point P^0 is

$$J = \begin{pmatrix} -\mu & 0 & -\frac{\beta(1-\eta)\delta S^0}{1+\alpha S^0} & -\frac{\beta(1-\eta)S^0}{1+\alpha S^0} & 0 & 0 \\ 0 & -(\mu+\sigma) & \frac{\beta(1-\eta)\delta S^0}{1+\alpha S^0} & \frac{\beta(1-\eta)S^0}{1+\alpha S^0} & 0 & 0 \\ 0 & (1-p)\sigma & -(\mu+\kappa+\xi) & 0 & 0 & 0 \\ 0 & p\sigma & \kappa & -(\mu+q+\gamma) & 0 & 0 \\ 0 & 0 & 0 & q & -(m+\mu) & 0 \\ 0 & 0 & \xi & \gamma & m & -\mu \end{pmatrix}.$$

Obviously, matrix J has three eigenvalues $\lambda_1 = -\mu$, $\lambda_2 = -(m+\mu)$ and $\lambda_3 = -\mu$, respectively. We only need to investigate the following matrix

$$J_1 = \begin{pmatrix} -(\mu+\sigma) & \frac{\beta(1-\eta)\delta S^0}{1+\alpha S^0} & \frac{\beta(1-\eta)S^0}{1+\alpha S^0} \\ (1-p)\sigma & -(\mu+\kappa+\xi) & 0 \\ p\sigma & \kappa & -(\mu+q+\gamma) \end{pmatrix}.$$

The characteristic equation of J_1 is

$$(\lambda+\mu+\sigma)(\lambda+\mu+\kappa+\xi)(\lambda+\mu+q+\gamma) = \frac{\beta(1-\eta)S^0}{1+\alpha S^0}\Big\{(1-p) \times\sigma[(\lambda+\mu+q+\gamma)\delta+\kappa] +p\sigma(\lambda+\mu+\kappa+\xi)\Big\}.$$

Denote $R_0 = R_{01} + R_{02} + R_{03}$, $D = \frac{\beta(1-\eta)S^0}{(1+\alpha S^0)(\mu+\sigma)}$, where

$$R_{01} = \frac{D(1-p)\sigma\delta}{\mu+\xi+\kappa}, \quad R_{02} = \frac{D(1-p)\sigma\kappa}{(\mu+\kappa+\xi)(\mu+q+\gamma)}, \quad R_{03} = \frac{Dp\sigma}{\mu+q+\gamma}.$$

Substituting R_{01}, R_{02}, R_{03} into above characteristic equation yields

$$\Big(\frac{\lambda}{\mu+\sigma}+1\Big)\Big(\frac{\lambda}{\mu+\kappa+\xi}+1\Big)\Big(\frac{\lambda}{\mu+q+\gamma}+1\Big) = R_{01}\frac{\lambda}{\mu+q+\gamma} +R_{03}\frac{\lambda}{\mu+\kappa+\xi} + R_0.$$

Suppose that the above equation has a root $\lambda_1 = x + iy$ with $x > 0$. When $R_0 < 1$, it is easy to prove that

$$\Big|\frac{\lambda}{\mu+\sigma}+1\Big| > 1, \ \Big|\Big(\frac{\lambda}{\mu+\kappa+\xi}+1\Big)\Big(\frac{\lambda}{\mu+q+\gamma}+1\Big)\Big| > \Big|R_{01}\frac{\lambda}{\mu+q+\gamma} + R_{03}\frac{\lambda}{\mu+\kappa+\xi} + R_0\Big|.$$

It follows that

$$\Big|\Big(\frac{\lambda}{\mu+\sigma}+1\Big)\Big(\frac{\lambda}{\mu+\kappa+\xi}+1\Big)\Big(\frac{\lambda}{\mu+q+\gamma}+1\Big)\Big| > \Big|R_{01}\frac{\lambda}{\mu+q+\gamma} + R_{03}\frac{\lambda}{\mu+\kappa+\xi} + R_0\Big|,$$

which yields contradiction. Hence, the eigenvalues of Jacobian matrix J all have negative real parts. Hence, the disease-free equilibrium P^0 is locally asymptotically stable by the Hurwitz criterion [25].

To investigate the global stability of the equilibrium P^0, we can construct the Lyapunov function as follows:

$$V(t) = E(t) + b_1 A(t) + b_2 I(t),$$

where $b_1 = \frac{\mu+\sigma}{(1-p)\sigma} - \frac{\beta(1-\eta)S^0 p\sigma}{(1+\alpha S^0)(\mu+q+\gamma)(1-p)\sigma}$, $b_2 = \frac{\beta(1-\eta)S^0}{(\mu+q+\gamma)(1+\alpha S^0)}$. The derivative of $V(t)$ along the system (1) satisfies

$$\begin{aligned}
\frac{dV}{dt} &= \frac{dE}{dt} + \Big[\frac{\mu+\sigma}{(1-p)\sigma} - \frac{\beta(1-\eta)S^0 p\sigma}{(1+\alpha S^0)(\mu+q+\gamma)(1-p)\sigma}\Big]\frac{dA}{dt} \\
&\quad + \frac{\beta(1-\eta)S^0}{(\mu+q+\gamma)(1+\alpha S^0)}\frac{dI}{dt} \\
&= \frac{\beta(1-\eta)S}{1+\alpha S}(I+\delta A) - (\mu+\sigma)E \\
&\quad + \Big[\frac{\mu+\sigma}{(1-p)\sigma} - \frac{\beta(1-\eta)S^0 p\sigma}{(1+\alpha S^0)(\mu+q+\gamma)(1-p)\sigma}\Big] \\
&\quad [(1-p)\sigma E - (\mu+\kappa+\xi)A] \\
&\quad + \frac{\beta(1-\eta)S^0}{(\mu+q+\gamma)(1+\alpha S^0)}[p\sigma E + \kappa A - (\mu+q+\gamma)I] \\
&\le \Big\{\frac{\beta(1-\eta)\delta S^0}{1+\alpha S^0} + \frac{\beta(1-\eta)\kappa S^0}{(\mu+q+\gamma)(1+\alpha S^0)} - (\mu+\kappa+\xi)\Big[\frac{\mu+\sigma}{(1-p)\sigma} \\
&\quad - \frac{\beta(1-\eta)p\sigma S^0}{(\mu+q+\gamma)(1+\alpha S^0)(1-p)\sigma}\Big]\Big\}A \\
&= \frac{\mu+\kappa+\xi}{(1-p)\sigma}\Big\{\frac{\beta(1-\eta)S^0}{1+\alpha S^0}\Big[\frac{(1-p)\sigma\delta}{\mu+\xi+\kappa} + \frac{(1-p)\sigma\kappa}{(\mu+\kappa+\xi)(\mu+q+\gamma)} \\
&\quad + \frac{p\sigma}{\mu+q+\gamma}\Big] - (\mu+\sigma)\Big\}A \\
&= \frac{(\mu+\kappa+\xi)(\mu+\sigma)}{(1-p)\sigma}(R_0 - 1)A.
\end{aligned}$$

When $R_0 < 1$, we can obtain that $\frac{dV}{dt} \le 0$. It is obvious that $\frac{dV}{dt} = 0$ if and only if $S = S^0$, $E = 0$, $A = 0$, $I = 0$, $Q = 0$, $R = 0$. Based on the LaSalle's Invariance Principle [26], we can conclude P^0 is globally asymptotically stable.

The global stability of disease-free equilibrium point is obtained by the sign of the first derivative of the Lyapunov function. Next, we will discuss the curvature by the sign of second derivative of the Lyapunov function.

$$\begin{aligned}
\frac{d^2V}{dt^2} &= \frac{d}{dt}\Big(\frac{dE}{dt} + b_1\frac{dA}{dt} + b_2\frac{dI}{dt}\Big) \\
&= \frac{\beta(1-\eta)(I+\delta A)}{(1+\alpha S)^2}S' + \frac{\beta(1-\eta)S}{(1+\alpha S)}(I'+\delta A') - (\mu+\sigma)E' \\
&\quad + b_1[(1-p)\sigma E' - (\mu+\kappa+\xi)A'] \\
&\quad + b_2[p\sigma E' + \kappa A' - (\mu+q+\gamma)I'] \\
&= \frac{\beta(1-\eta)S}{(1+\alpha S)}[p\sigma E + \kappa A - (\mu+q+\gamma)I
\end{aligned}$$

$$
\begin{aligned}
&+\delta(1-p)\sigma E-\delta(\mu+\kappa+\xi)A]\\
&+\frac{\beta(1-\eta)(I+\delta A)}{(1+\alpha S)^2}\Big[\Lambda-\frac{\beta(1-\eta)S}{(1+\alpha S)}(I+\delta A)-\mu S\Big]\\
&-(\mu+\sigma)\Big[\frac{\beta(1-\eta)S}{(1+\alpha S)}(I+\delta A)-(\mu+\sigma)E\Big]\\
&+b_1\Big\{(1-p)\sigma\Big[\frac{\beta(1-\eta)S}{(1+\alpha S)}(I+\delta A)-(\mu+\sigma)E\Big]\\
&-(\mu+\kappa+\xi)[(1-p)\sigma E-(\mu+\kappa+\xi)A]\Big\}\\
&+b_2\Big\{p\sigma\Big[\frac{\beta(1-\eta)S}{(1+\alpha S)}(I+\delta A)-p\sigma(\mu+\sigma)E\Big]\\
&+\kappa[(1-p)\sigma E-(\mu+\kappa+\xi)A]\\
&-(\mu+q+\gamma)[p\sigma E+\kappa A-(\mu+q+\gamma)I]\Big\}.
\end{aligned}
$$

For convenience, we can put together positive and negative part and rewrite the above equality as follows

$$\frac{d^2V}{dt^2}=\Omega_1-\Omega_2.$$

Therefore, if $\Omega_1>\Omega_2$, $\frac{d^2V}{dt^2}>0$ means that the Lyapunov function V has a local minimum value. If $\Omega_1<\Omega_2$, $\frac{d^2V}{dt^2}<0$ suggests that the Lyapunov function V has a local maximum value. Otherwise, if $\Omega_1=\Omega_2$, $\frac{d^2V}{dt^2}=0$ implies that there is a disease-free equilibrium point.

The threshold result in Theorem 1 implies that the number of the infected population will gradually become lower and lower if $R_0<1$. If $R_0>1$, the solutions start from nearly to P^0 are far from P^0. This implies that P^0 is unstable. When $R_0>1$, the instability of P^0 implies uniform persistence of model (1).

Theorem 2. *When $R_0>1$, the disease will keep persistent in the population, then the model (1) is uniformly persistent.*

Proof. Since the equation

$$\frac{dS}{dt}=\Lambda-\mu S, \tag{2}$$

has a positive equilibrium $S^0=\frac{\Lambda}{\mu}$, which is globally attractive.

When $R_0>1$, we consider the following perturbed system

$$\frac{dS}{dt}=\Lambda-\mu S-\theta\frac{\beta(1-\eta)(1+\delta)S}{1+\alpha S}. \tag{3}$$

Due to the equilibrium $S^0=\frac{\Lambda}{\mu}$ is globally attractive, hence, we can choose a small $\theta>0$ such that the system exists a unique positive equilibrium $S^0(\theta)$, which is globally asymptotically stable. Since $S^0(\theta)$ is a continuous function of θ and $\frac{S}{1+\alpha S}$ is a monotonically increasing function. Consequently, there exists an enough small positive number ε such that $\frac{S^0(\theta)}{1+\alpha S^0(\theta)}>\frac{S^0}{1+\alpha S^0}-\varepsilon$.

We claim that $\limsup_{t\to\infty}(E(t),A(t),I(t))>\theta$. Otherwise, we suppose the contrary, there exists small enough number $\zeta>0$ ($\zeta<\theta$) and positive number $T>0$ such that $E(t)<\zeta$, $A(t)<\zeta$, $I(t)<\zeta$ for all $t>T$. From model (1), we can obtain

$$\frac{dS}{dt}\geq\Lambda-\mu S-\frac{\beta(1-\eta)(\zeta+\delta\zeta)S}{1+\alpha S}\geq\Lambda-\mu S-\theta\frac{\beta(1-\eta)(1+\delta)S}{1+\alpha S}.$$

Due to the equilibrium $S^0(\theta)$ of inequality (3) is globally attractive, and $\frac{S^0(\theta)}{1+\alpha S^0(\theta)}>\frac{S^0}{1+\alpha S^0}-\varepsilon$. Using the comparison principle, there exists a positive number $T_1>T>0$, such that $\frac{S(t)}{1+\alpha S(t)}>\frac{S^0}{1+\alpha S^0}-\varepsilon$ for all $t>T_1$.

For any small number $\varepsilon>0$, when $t>T_1$, we can obtain that

$$\begin{cases}\frac{dE}{dt}\geq\beta(1-\eta)\Big(\frac{S^0}{1+\alpha S^0}-\varepsilon\Big)(I+\delta A)-(\mu+\sigma)E,\\ \frac{dA}{dt}=(1-p)\sigma E-(\mu+\kappa+\xi)A,\\ \frac{dI}{dt}=p\sigma E+\kappa A-(\mu+q+\gamma)I.\end{cases}$$

We consider the following auxiliary system

$$\begin{cases}\frac{dE_1}{dt}=\beta(1-\eta)\Big(\frac{S^0}{1+\alpha S^0}-\varepsilon\Big)(I_1+\delta A_1)-(\mu+\sigma)E_1,\\ \frac{dA_1}{dt}=(1-p)\sigma E_1-(\mu+\kappa+\xi)A_1,\\ \frac{dI_1}{dt}=p\sigma E_1+\kappa A_1-(\mu+q+\gamma)I_1.\end{cases} \tag{4}$$

The coefficient matrix of system (4) is

$$J(\varepsilon)=\begin{pmatrix}-(\mu+\sigma) & \beta(1-\eta)\Big(\frac{S^0}{1+\alpha S^0}-\varepsilon\Big)\delta & \beta(1-\eta)\Big(\frac{S^0}{1+\alpha S^0}-\varepsilon\Big)\\ (1-p)\sigma & -(\mu+\kappa+\xi) & 0\\ p\sigma & \kappa & -(\mu+q+\gamma)\end{pmatrix}.$$

When $R_0>1$, the coefficient matrix $J(0)$ at least exists one positive eigenvalue, namely $\rho(J(0))>0$. Since $\rho(J(0))>0$ is continuous about small ε. Hence, there exists a sufficiently small $\varepsilon>0$ satisfying $\rho(J(\varepsilon))>0$. This implies that the solutions of auxiliary system (4) satisfy $E_1(t),A_1(t),I_1(t)\to+\infty$ as $t\to+\infty$. Using the comparison theorem, we conclude $\lim_{t\to\infty}E(t)=\infty$, $\lim_{t\to\infty}A(t)=\infty$, $\lim_{t\to\infty}I(t)=\infty$. Which contracts with previous hypothesis, this implies the conclusion $\limsup_{t\to\infty}(E(t),A(t),I(t))>\theta$ holds true.

Define the sets

$$X=\Omega=\Big\{(S,E,A,I,Q,R)\in\mathbb{R}^6_+\mid S+E+A+I+Q+R\leq\frac{\Lambda}{\mu}\Big\},$$
$$X_0=\{(S,E,A,I,Q,R)\in X\mid E>0,\ A>0,\ I>0\},\qquad \partial X_0=X\backslash X_0.$$

Obviously, X is a compact and positive invariant set of model (1). Then X_0 is uniformly and ultimately bounded, ∂X_0 is closed with respect to X. As a result, model (1) is compact and point dissipative.

Let

$$M_\partial=\{(S,E,A,I,Q,R)\in\partial X_0\mid(S(t),E(t),A(t),I(t),Q(t),R(t))\in\partial X_0,\ \forall t\geq0\}.$$

We can prove that $M_\partial=\{(S,0,0,0,0,0)\mid S(t)\geq0\}$. Due to the definition of M_∂, we can obtain $\{(S,0,0,0,0,0)\in\partial X_0\mid S(t)\geq0\}\subset M_\partial$. Suppose $(S(0),E(0),A(0),I(0),Q(0),R(0))\in M_\partial$, we can conclude $E(t)=0,A(t)=0,I(t)=0$ for all $t>0$. If not, at least one of $E(t),A(t),I(t)$ is positive. Without loss of generality, we assume there exists $t_0>0$ such that $E(t)>0$, $A(t)=0$, $I(t)=0$ for any $t>t_0$.

Form the equations of model (1), we can obtain the following equations:

$$\begin{cases}\frac{dA}{dt}=(1-p)\sigma E-(\mu+\kappa+\xi)A=(1-p)\sigma E,\\ \frac{dI}{dt}=p\sigma E+\kappa A-(\mu+q+\gamma)I=p\sigma E.\end{cases}$$

There exists a small enough number $\omega>0$ such that $A(t)>0$, $I(t)>0$ when $t_0<t<t_0+\omega$. Namely, the solution $(S(t),E(t),A(t),I(t),Q(t),R(t))\notin\partial X_0$. This contradiction implies that $(S(0),E(0),A(0),I(0),Q(0),R(0))\in M_\partial$ only if $E(0)=0$, $A(0)=0$, $I(0)=0$, that is $M_\partial\subset\{(S,0,0,0,0,0)\in\partial X_0\mid S(t)\geq0\}$. Hence, $M_\partial=\{(S,0,0,0,0,0)\in\partial X_0\mid S(t)\geq0\}$.

When $R_0>1$, the only disease-free equilibrium point P^0 is unstable in ∂X_0. By using Lemma 5.9 in research [27], we claim that no subset of P^0 forms a cycle in ∂X_0. P^0 is an isolated invariant set in X. Namely $W^s(P^0)\cap X_0=\varnothing$. Every trajectory of set M_∂ converges to P^0 and P^0 is aperiodic in M_∂. From Theorem 1.3.1 and Remark 1.3.1 in Ref. [28],

we can conclude that the solutions of model (1) are uniformly persistent with respect to $(X_0, \partial X_0)$.

The stability of the endemic equilibrium

If $R_0 > 1$, it can be demonstrated that model (1) may admit a unique endemic equilibrium $P^*(S^*, E^*, A^*, I^*, Q^*, R^*)$, which satisfies that

$$\begin{cases} \Lambda - \dfrac{\beta(1-\eta)}{1+\alpha S^*} S^*(I^* + \delta A^*) - \mu S^* = 0, \\ \dfrac{\beta(1-\eta)}{1+\alpha S^*} S^*(I^* + \delta A^*) - (\mu+\sigma)E^* = 0, \\ (1-p)\sigma E^* - (\mu+\kappa+\xi)A^* = 0, \\ p\sigma E^* + \kappa A^* - (\mu+q+\gamma)I^* = 0, \\ qI^* - (m+\mu)Q^* = 0, \\ \xi A^* + \gamma I^* + mQ^* - \mu R^* = 0. \end{cases}$$

By straightforward calculations, one can have that

$$S^* = \frac{S^0}{\alpha(R_0-1)S^0 + R_0}, \quad E^* = \frac{\Lambda - \dfrac{\mu S^0}{\alpha(R_0-1)S^0 + R_0}}{\mu+\sigma},$$
$$I^* = \frac{p\sigma E^* + \kappa A^*}{\mu+q+\gamma},$$
$$A^* = \frac{(\Lambda - \dfrac{\mu S^0}{\alpha(R_0-1)S^0 + R_0})(1-p)\sigma}{(\mu+\sigma)(\mu+\kappa+\xi)}, \quad Q^* = \frac{qI^*}{m+\mu},$$
$$R^* = \frac{\gamma I^* + \xi A^* + mQ^*}{\mu}.$$

Theorem 3. *Assume that $R_0 > 1$, then the endemic equilibrium $P^*(S^*, E^*, A^*, I^*, Q^*, R^*)$ of model (1) is globally asymptotically stable.*

Proof. The linearized matrix of model (1) at the endemic equilibrium point P^* is

$$J_2 = \begin{pmatrix} -X-\mu & 0 & -Y\delta & -Y & 0 & 0 \\ X & -(\mu+\sigma) & Y\delta & Y & 0 & 0 \\ 0 & (1-p)\sigma & -(\mu+\kappa+\xi) & 0 & 0 & 0 \\ 0 & p\sigma & \kappa & -(\mu+q+\gamma) & 0 & 0 \\ 0 & 0 & 0 & q & -(m+\mu) & 0 \\ 0 & 0 & \xi & \gamma & m & -\mu \end{pmatrix},$$

where we denote $X = \dfrac{\beta(1-\eta)(I^* + \delta A^*)}{(1+\alpha S^*)^2}$ and $Y = \dfrac{\beta(1-\eta)S^*}{1+\alpha S^*}$.

The characteristic equation of J_2 is

$$(\lambda+\mu)(\lambda+m+\mu)[(\lambda+X+\mu)(\lambda+\mu+\sigma)(\lambda+\mu+\kappa+\xi)(\lambda+\mu+q+\gamma)$$
$$+XYZ - Y(\lambda+X+\mu)Z] = 0,$$

where $Z = (\lambda+\mu+q+\gamma)(1-p)\sigma\delta + p\sigma(\lambda+\mu+\kappa+\xi) + (1-p)\sigma\kappa$. It is obvious that the above characteristic equation has two negative real root $-\mu$, $-m-\mu$ and other roots are determined by the following equation

$$(\lambda+X+\mu)(\lambda+\mu+\sigma)(\lambda+\mu+\kappa+\xi)(\lambda+\mu+q+\gamma) = (\lambda+\mu)YZ. \tag{5}$$

Noting that

$$Y\left\{\frac{p\sigma}{\mu+q+\gamma} + \frac{(1-p)\sigma\kappa}{(\mu+\kappa+\xi)(\mu+q+\gamma)} + \frac{(1-p)\sigma\delta}{\mu+\xi+\kappa}\right\} = \mu+\sigma.$$

Denote that $\widetilde{R_{01}} = \dfrac{Yp\sigma}{(\mu+\sigma)(\mu+q+\gamma)}$, $\widetilde{R_{02}} = \dfrac{Y(1-p)\sigma\kappa}{(\mu+\sigma)(\mu+\kappa+\xi)(\mu+q+\gamma)}$, $\widetilde{R_{03}} = \dfrac{Y(1-p)\sigma\delta}{(\mu+\sigma)(\mu+\xi+\kappa)}$. Then, $\widetilde{R_{01}} + \widetilde{R_{02}} + \widetilde{R_{03}} = 1$. Substituting $\widetilde{R_{01}}, \widetilde{R_{02}}, \widetilde{R_{03}}$ into Eq. (5) yields

$$(\lambda+X+\mu)\Big(\frac{\lambda}{\mu+\sigma}+1\Big)\Big(\frac{\lambda}{\mu+q+\gamma}+1\Big)\Big(\frac{\lambda}{\mu+\kappa+\xi}+1\Big)$$
$$= (\lambda+\mu)\Big(\frac{\lambda\widetilde{R_{01}}}{\mu+q+\gamma} + \frac{\lambda\widetilde{R_{03}}}{\mu+\kappa+\xi} + 1\Big).$$

Provided that Eq. (5) has a root $\lambda_2 = a + ib$ with $a > 0$, we can obtain

$$\Big|\frac{\lambda}{\mu+\sigma}+1\Big| > 1, \quad |\lambda+X+\mu| > |\lambda+\mu|,$$

$$\Big|\frac{\lambda}{\mu+\kappa+\xi}+1\Big|\Big|\frac{\lambda}{\mu+q+\gamma}+1\Big| > \Big|\frac{\lambda\widetilde{R_{01}}}{\mu+q+\gamma} + \frac{\lambda\widetilde{R_{03}}}{\mu+\kappa+\xi}+1\Big|.$$

Therefore, we can conclude that

$$|\lambda+X+\mu|\Big|\frac{\lambda}{\mu+\sigma}+1\Big|\Big|\frac{\lambda}{\mu+\kappa+\xi}+1\Big|\Big|\frac{\lambda}{\mu+q+\gamma}+1\Big|$$
$$> |\lambda+\mu|\Big|\frac{\lambda\widetilde{R_{01}}}{\mu+q+\gamma} + \frac{\lambda\widetilde{R_{03}}}{\mu+\kappa+\xi}+1\Big|,$$

which contradicts to Eq. (5). Namely, all roots of Eq. (5) have negative real parts. P^* is locally asymptotically stable by the Hurwitz criterion [25].

To investigate the globally asymptotically stable of endemic equilibrium P^*, we suppose the following Lyapunov function as

$$U(t) = V_1(t) + c_1V_2(t) + c_2V_3(t),$$

whereas $V_1 = \int_{S^*}^{S} \dfrac{F(x)-F(S^*)}{F(x)}dx + E - E^* - E^*\ln\dfrac{E}{E^*}$, $V_2 = A - A^* - A^*\ln\dfrac{A}{A^*}$, $V_3 = I - I^* - I^*\ln\dfrac{I}{I^*}$, and $F(x) = \dfrac{\beta(1-\eta)}{1+\alpha x}x$. Constants c_1 and c_2 will be determined later. Calculating the derivative of V_i, $i = 1, 2, 3$, along positive solutions of model (1) yields:

$$\begin{aligned} \frac{dV_1}{dt} &= \Big(1 - \frac{F(S^*)}{F(S)}\Big)\frac{dS}{dt} + \Big(1 - \frac{E^*}{E}\Big)\frac{dE}{dt} \\ &= \Big(1 - \frac{F(S^*)}{F(S)}\Big)[\mu S^* + F(S^*)(I^* + \delta A^*) - \mu S - F(S)(I + \delta A)] \\ &\quad + \Big(1 - \frac{E^*}{E}\Big)\Big[F(S)(I+\delta A) - F(S^*)(I^* + \delta A^*)\frac{E}{E^*}\Big] \\ &= \Big(1 - \frac{F(S^*)}{F(S)}\Big)\Big[\mu(S^* - S) + F(S^*)I^*\Big(1 - \frac{F(S)I}{F(S^*)I^*}\Big) \\ &\quad + F(S^*)\delta A^*\Big(1 - \frac{F(S)\delta A}{F(S^*)\delta A^*}\Big)\Big] \\ &\quad + \Big(1 - \frac{E^*}{E}\Big)\Big[F(S^*)I^*\Big(\frac{F(S)I}{F(S^*)I^*} - \frac{E}{E^*}\Big) \\ &\quad + F(S^*)\delta A^*\Big(\frac{F(S)\delta A}{F(S^*)\delta A^*} - \frac{E}{E^*}\Big)\Big] \\ &\le F(S^*)I^*\Big[2 - \frac{E}{E^*} - \frac{E^*F(S)I}{EF(S^*)I^*} - \frac{F(S^*)}{F(S)} + \frac{I}{I^*}\Big] \\ &\quad + F(S^*)\delta A^*\Big[2 - \frac{E}{E^*} - \frac{E^*F(S)A}{EF(S^*)A^*} - \frac{F(S^*)}{F(S)} + \frac{A}{A^*}\Big] \\ &= F(S^*)I^*\Big[1 - \frac{F(S^*)}{F(S)} + \ln\frac{F(S^*)}{F(S)} - \ln\frac{F(S^*)}{F(S)} + 1 - \frac{E^*F(S)I}{EF(S^*)I^*} \\ &\quad + \ln\frac{E^*F(S)I}{EF(S^*)I^*} - \ln\frac{E^*F(S)I}{EF(S^*)I^*} - \frac{E}{E^*} + \frac{I}{I^*}\Big] \\ &\quad + F(S^*)\delta A^*\Big[1 - \frac{F(S^*)}{F(S)} + \ln\frac{F(S^*)}{F(S)} - \ln\frac{F(S^*)}{F(S)} + 1 - \frac{E^*F(S)A}{EF(S^*)A^*} \\ &\quad + \ln\frac{E^*F(S)A}{EF(S^*)A^*} - \ln\frac{E^*F(S)A}{EF(S^*)A^*} - \frac{E}{E^*} + \frac{A}{A^*}\Big] \\ &\le F(S^*)I^*\Big(-\frac{E}{E^*} + \ln\frac{E}{E^*} + \frac{I}{I^*} - \ln\frac{I}{I^*}\Big) \\ &\quad + F(S^*)\delta A^*\Big(-\frac{E}{E^*} + \ln\frac{E}{E^*} + \frac{A}{A^*} - \ln\frac{A}{A^*}\Big). \end{aligned}$$

$$\begin{aligned} \frac{dV_2}{dt} &= \Big(1 - \frac{A^*}{A}\Big)\Big[(1-p)\sigma E - \frac{(1-p)\sigma E^*}{A^*}A\Big] \\ &= (1-p)\sigma E^*\Big(1 - \frac{A^*}{A}\Big)\Big(\frac{E}{E^*} - \frac{A}{A^*}\Big) \\ &= (1-p)\sigma E^*\Big(1 - \frac{A^*E}{AE^*} + \ln\frac{A^*E}{AE^*} - \ln\frac{A^*E}{AE^*} + \frac{E}{E^*} - \frac{A}{A^*}\Big) \\ &\le (1-p)\sigma E^*\Big(\frac{E}{E^*} - \ln\frac{E}{E^*} - \frac{A}{A^*} + \ln\frac{A}{A^*}\Big). \end{aligned}$$

$$\begin{aligned} \frac{dV_3}{dt} &= \Big(1 - \frac{I^*}{I}\Big)\Big[p\sigma E + \kappa A - \frac{p\sigma E^* + \kappa A^*}{I^*}I\Big] \\ &= \Big(1 - \frac{I^*}{I}\Big)\Big[p\sigma E^*\Big(\frac{E}{E^*} - \frac{I}{I^*}\Big) + \kappa A^*\Big(\frac{A}{A^*} - \frac{I}{I^*}\Big)\Big] \end{aligned}$$

$$
\begin{aligned}
&= p\sigma E^*\Big(1-\frac{I^*}{I}\Big)\Big(\frac{E}{E^*}-\frac{I}{I^*}\Big)+\kappa A^*\Big(1-\frac{I^*}{I}\Big)\Big(\frac{A}{A^*}-\frac{I}{I^*}\Big)\\
&\le p\sigma E^*\Big(-\frac{I}{I^*}+\ln\frac{I}{I^*}+\frac{E}{E^*}-\ln\frac{E}{E^*}\Big)\\
&\quad+\kappa A^*\Big(-\frac{I}{I^*}+\ln\frac{I}{I^*}+\frac{A}{A^*}-\ln\frac{A}{A^*}\Big).
\end{aligned}
$$

We choose

$$
c_1=\frac{F(S^*)\delta A^*+\dfrac{F(S^*)I^*}{p\sigma E^*+\kappa A^*}\kappa A^*}{(1-p)\sigma E^*},\quad c_2=\frac{F(S^*)I^*}{p\sigma E^*+\kappa A^*}.
$$

Hence, according to the above inequalities, direct calculation shows that

$$
\begin{aligned}
\frac{dU}{dt} &= \frac{dV_1}{dt}+\frac{F(S^*)\delta A^*+\dfrac{F(S^*)I^*}{p\sigma E^*+\kappa A^*}\kappa A^*}{(1-p)\sigma E^*}\frac{dV_2}{dt}+\frac{F(S^*)I^*}{p\sigma E^*+\kappa A^*}\frac{dV_3}{dt}\\
&\le F(S^*)I^*\Big(-\frac{E}{E^*}+\ln\frac{E}{E^*}+\frac{I}{I^*}-\ln\frac{I}{I^*}\Big)\\
&\quad+F(S^*)\delta A^*\Big(-\frac{E}{E^*}+\ln\frac{E}{E^*}+\frac{A}{A^*}-\ln\frac{A}{A^*}\Big)\\
&\quad+\frac{F(S^*)\delta A^*+\dfrac{F(S^*)I^*}{p\sigma E^*+\kappa A^*}\kappa A^*}{(1-p)\sigma E^*}\\
&\quad\times(1-p)\sigma E^*\Big(\frac{E}{E^*}-\ln\frac{E}{E^*}-\frac{A}{A^*}+\ln\frac{A}{A^*}\Big)\\
&\quad+\frac{F(S^*)I^*}{p\sigma E^*+\kappa A^*}\Big[p\sigma E^*\Big(-\frac{I}{I^*}+\ln\frac{I}{I^*}+\frac{E}{E^*}-\ln\frac{E}{E^*}\Big)\\
&\quad+\kappa A^*\Big(-\frac{I}{I^*}+\ln\frac{I}{I^*}+\frac{A}{A^*}-\ln\frac{A}{A^*}\Big)\Big]\\
&= 0.
\end{aligned}
$$

Thus, it follows from the inequality of arithmetic means that $\frac{dU}{dt}\le 0$, and $\frac{dU}{dt}=0$ holding if and only if $S=S^*$, $E=E^*$, $A=A^*$, $I=I*$, $Q=Q^*$, $R=R^*$. It can be proved that $M=\{P^*\}$ is the largest invariant subset of $\Big\{(S(t),E(t),A(t),I(t),Q(t),R(t)) : \frac{dU}{dt}=0\Big\}$. Consequently, we obtain that P^* is the globally asymptotically stable from LaSalle's invariance principle [26].

The global stability of endemic equilibrium point is obtained by the sign of the first derivative of the Lyapunov function. Next, we will discuss the curvature by the sign of second derivative of the Lyapunov function.

$$
\begin{aligned}
\frac{d^2U}{dt^2} &= \frac{d}{dt}\Big(\frac{dV_1}{dt}+c_1\frac{dV_2}{dt}+c_2\frac{dV_3}{dt}\Big)\\
&= \frac{d}{dt}\Big[\Big(1-\frac{F(S^*)}{F(S)}\Big)\frac{dS}{dt}+\Big(1-\frac{E^*}{E}\Big)\frac{dE}{dt}\Big]\\
&\quad+c_1\Big(1-\frac{A^*}{A}\Big)\frac{dA}{dt}+c_2\Big(1-\frac{I^*}{I}\Big)\frac{dI}{dt}\\
&= \frac{F(S^*)F'(s)}{F^2(s)}S'+\Big(1-\frac{F(S^*)}{F(S)}\Big)S''+\Big(\frac{E'}{E}\Big)^2E^*+\Big(1-\frac{E^*}{E}\Big)E''\\
&\quad+c_1\Big[\Big(\frac{A'}{A}\Big)^2A^*+\Big(1-\frac{A^*}{A}\Big)A''\Big]+c_2\Big[\Big(\frac{I'}{I}\Big)^2I^*+\Big(1-\frac{I^*}{I}\Big)I''\Big].
\end{aligned}
$$

Based on the derivation rules for compound function, we can know

$$
S''=-\frac{F(S)(I+\delta A)}{S(1+\alpha S)}S'-F(S)(I'+\delta A')-\mu S',
$$

$$
E''=\frac{F(S)(I+\delta A)}{S(1+\alpha S)}S'+F(S)(I'+\delta A')-(\mu+\sigma)E',
$$

$$
A''=(1-p)\sigma E'-(\mu+\kappa+\xi)A',\quad I''=p\sigma E'+\kappa A'-(\mu+q+\gamma)I'.
$$

Then, we can deduce that

$$
\begin{aligned}
\frac{d^2U}{dt^2} &= \frac{F(S^*)F'(s)}{F^2(s)}S'+\Big(1-\frac{F(S^*)}{F(S)}\Big)\\
&\quad\times\Big[-\frac{F(S)(I+\delta A)}{S(1+\alpha S)}S'-F(S)(I'+\delta A')-\mu S'\Big]\\
&\quad+\Big(\frac{E'}{E}\Big)^2E^*+\Big(1-\frac{E^*}{E}\Big)\\
&\quad\times\Big[\frac{F(S)(I+\delta A)}{S(1+\alpha S)}S'+F(S)(I'+\delta A')-(\mu+\sigma)E'\Big]\\
&\quad+\frac{F(S^*)\delta A^*+\dfrac{F(S^*)I^*}{p\sigma E^*+\kappa A^*}\kappa A^*}{(1-p)\sigma E^*}\Big(\frac{A'}{A}\Big)^2A^*\\
&\quad+\frac{F(S^*)I^*}{p\sigma E^*+\kappa A^*}\Big(\frac{I'}{I}\Big)^2I^*\\
&\quad+\frac{F(S^*)\delta A^*+\dfrac{F(S^*)I^*}{p\sigma E^*+\kappa A^*}\kappa A^*}{(1-p)\sigma E^*}\Big(1-\frac{A^*}{A}\Big)\\
&\quad\times\Big[(1-p)\sigma E'-(\mu+\kappa+\xi)A'\Big]\\
&\quad+\frac{F(S^*)I^*}{p\sigma E^*+\kappa A^*}\Big(1-\frac{I^*}{I}\Big)\Big[p\sigma E'+\kappa A'-(\mu+q+\gamma)I'\Big].
\end{aligned}
$$

Next, we substitute the derivative formula of S', E', A', I' into the above equality. For convenience, we can put together positive and negative part and rewrite the above equality as follows

$$
\frac{d^2U}{dt^2}=\Omega_{11}-\Omega_{12}.
$$

Therefore, if $\Omega_{11}>\Omega_{12}$, $\frac{d^2U}{dt^2}>0$ means that the Lyapunov function U has a local minimum value. However, if $\Omega_{11}<\Omega_{12}$, $\frac{d^2U}{dt^2}<0$ suggests that the Lyapunov function U has a local maximum value. While if $\Omega_{11}=\Omega_{12}$, $\frac{d^2U}{dt^2}=0$ implies that there is an endemic equilibrium point.

Data fitting and sensitivity analysis

Data fitting

In the following part, we will fit the data of the cumulative confirmed cases of COVID-19 in New York City by Markov-Chain Monte-Carlo(MCMC) simulations. Under the ongoing COVID-19 pandemic, responses and suggestions regarding the mask use have varied greatly by the public. There has been a major change about the government's response to COVID-19 in NYC, i.e., the government urged the public to stay at home on March 20, 2020, and announced the gradual re-opening since July 7, 2020, and then the US CDC announced governors to be prepared for COVID-19 vaccine distribution by 1st November, 2020 [29]. Based on the policies, we collected the data about the number of daily and cumulative confirmed cases of New York City from March 26 to October 31, 2020 from the Johns Hopkins University [6]. Hence, the transmission of COVID-19 in NYC can be divided into three stages based on the government's different policies. The first stage is from March 20 to April 03, 2020, due to the shortage of medical resources, especially in the supply of masks, there are not enough masks for ordinary people, the percentage of people wearing masks was very low. The second stage is from April 04 to June 07, 2020, the proportion of people wearing masks has increased relatively and most people are quarantined at home. The third stage is from June 08 to October 31, 2020, the society is reopening and the contact between people became frequent. We will simulate the daily and cumulative confirmed cases of New York City for the period from March 20 to October 31, 2020 by using model (1). Here, $C(t)$ represents the cumulative number of cases,

$$
\frac{dC(t)}{dt}=p\sigma E(t)+\kappa A(t).
$$

We assume and calculate some parameters apart from β, α and κ, which are showed in Table 2. The total number of population in New York City is 8 804 190 [30]. The initial values are given by $C(0)=10\,532$, $S(0)=8\,763\,090$, $E(0)=16\,000$, $A(0)=7300$, $I(0)=8000$, $Q(0)=800$, $R(0)=9000$ [6,30]. $E(0)$, $A(0)$, $I(0)$ are estimated by the fitting. In the early stage of the epidemic, few people in the public wear masks in the liberal and democratic society of the United States and

Table 2
Estimated parameters values with respect to COVID-19 cases.

Variables	Likely range	Default value	Reference
Λ		300	[30]
μ		0.00002245 day^{-1}	[30]
η	0–1	0.5	[17]
δ	0.1–0.6	0.25	[7,13,31]
σ	1/7–1/4.1 days	1/5.2 day^{-1}	[32]
p	0.15–0.7	0.5	[7,13,31]
ξ	1/14–1/3 day^{-1}	1/7 day^{-1}	[7,33]
q	0.02–0.1	0.075 day^{-1}	[31,33]
γ	1/30–1/3 day^{-1}	1/9 day^{-1}	[7,33]
m	1/30–1/3 day^{-1}	1/14 day^{-1}	[7,33]

we suppose there were no intervention measures. The protective effect of wearing masks on the disease has been controversial, and people who wear masks are regarded as disseminators of the virus. Some people are afraid of wearing masks for fear of opposition. Steffen [7] derived the relationship between mask coverage and the transmission rate is similarly linear, and found that masks are useful with respect to both preventing disease in healthy person and asymptomatic infection.

The coverage rate of mask use is about 10 percent of the population in the early stage of the USA State according to the survey from the website [34]. In order to estimate the value of parameter β and κ, the effective coverage rate of wearing masks α is supposed 0.1 in the first stage. Next we make the Latin Hypercube Sampling and MCMC simulations based on the algorithm similar to research [35–37]. Using 10 000 times simulation, we can receive the parameter value for β and κ with MCMC chain in Fig. 3. Then the mean value, the standard deviation, MCMC error and Geweke for parameter β and κ are illustrated in Table 3. It is easy to see that the Markov-chain of parameters β and κ are converged from Fig. 3. The US CDC advised the public to wear masks on 03 April, 2020 [7] and medical resources were relatively abundant, many people began to wear masks in public. In order to estimate the effective coverage rate of wearing masks by the public in the second stage, namely the value of parameter α, other parameters are the same as the first stage. We still apply the Latin Hypercube Sampling and MCMC simulation to estimate it and can acquire the parameter value of α with Markov chain in Fig. 4. The mean value, the standard deviation, MCMC error and Geweke for parameter α is demonstrated in Table 3. After gradual reopening since June 7, 2020, the contact became frequent in the public and the transmission rate increased. So as to estimate the transmission rate β, we still utilize the MCMC method to calculate it. The Markov chain of parameter β of the third stage is showed in Fig. 5, and the mean value, the standard deviation, MCMC error and Geweke for parameter β are presented in Table 3. Cumulative infection cases, daily new infected cases predicted and comparison with the confirmed cases for the first stage, second stage and third stage are demonstrated in Fig. 6(a) (b) (c), and which also exhibit the 95% percent interval and the median of these simulation outputs. It can be observed that the cumulative infected cases predicted by model (1) are nearly agreement with the notifiable reported cases. The red circles show the number of actual confirmed cases and the blue solid curve indicates the predicted actual confirmed cases of the model. The red solid curve expresses the number of new daily confirmed cases, the blue dotted curve represents the predicted daily new cases of the model. Based on the fitting result, we can roughly estimate the mean effective reproduction number $R_0 = 1.822$ in the first stage, which means that COVID-19 will become an endemic in New York City without any further control measures in the first stage. Nevertheless, the effective reproduction number $R_0 = 0.6483$ in the second stage, $R_0 = 1.024$ in the third stage. This means that the enlarging use of masks and home quarantine in the second stage played an important role in controlling the spread of COVID-19 in New York City. With the gradual reopening in the third stage, the spread of COVID-19 cannot be restrained by wearing masks alone. A combination of vaccine and other control measures is required.

Table 3
Parameter estimation for β , κ and α with the method of MCMC.

Stage	Parameter	Mean	Standard	MC error	Geweke
First	β	0.0748	0.000246	7.72e−05	0.9922
	κ	0.3616	0.036643	0.0011	0.9791
Second	α	0.2813	0.0007556	1.4597e−05	0.9996
Third	β	0.1184	0.000878	1.528e−05	0.9989

Table 4
Partial rank correlation coefficients (PRCC) of R_0 in three stages.

Parameter	PRCC of the first stage/ second stage/third stage	P-value of the first stage/ second stage/third stage
α	−0.8577/−0.9706/−0.9041	0/0
β	0.9189/0.8328/0.9828	0/0
σ	0.0374/0.02922/0.0443	0.2396/0.3581/0.1634
δ	0.3038/0.2235/0.1181	0/0/0.0002
p	0.6681/0.4797/0.5353	0/0/0
ξ	−0.1621/−0.0922/−0.2952	0/0.0036/0
κ	0.1797/0.1236/0.02145	0/0/0.5001/
q	−0.6284/−0.4791/−0.3009	0/0/0
η	−0.9151/−0.8316/−0.5918	0/0/0
γ	−0.6102/−0.4452/−0.2463	0/0/0

Sensitivity analysis

Since most parameters used in above simulation are uncertain, the uncertainty and sensitivity analysis of these parameters are required to find out the decisive parameters of R_0 and to further verify the correctness of the model. The PRCC-based sensitivity analysis evaluates the influence of parameters on the response function of basic reproduction number R_0. Here, PRCC values of some parameters are given based on Latin Hypercube Sampling [37]. We take the sample size $N = 10\,000$, in addition to Λ, μ, all parameters as the input variables, the value of R_0 as output variables. We assume that all parameters are uniformly distributed and the significant level is selected as 0.01. If P-value is smaller than 0.01, which is considered significant. The partial rank correlation coefficients about R_0 in the first and second stage were calculated in Table 4. Fig. 7 (a) shows the PRCC histogram of some parameters about R_0 in the first stage with $\alpha = 0.1$, Fig. 7(b) illustrates the PRCC histogram about R_0 in the second stage with $\alpha = 0.281$, and Fig. 7(c) demonstrates the PRCC histogram about R_0 in the third stage with $\beta = 0.1184$. It can be observed that the parameter σ is not sensitive in three stages, while κ is sensitive in the front two stages, but not sensitive in the third stage. The transmission rate β, the effective coverage rate of mask use α, the rate of keeping social distance η and the admission rate q have significant effect on the basic reproduction number R_0. These parameters which can typically be influenced by the control measures. The results suggest that the most relevant factors in COVID-19 transmission and in the elevation of the number of infected cases are the protective effect and the proportion of mask use.

To ascertain the dependence of R_0 on controllable parameters β, α, δ, p, q, κ, η, γ in three stages, we take the parameter values as in Tables 2 and 3. By changing two parameters of R_0 and fixing other parameters, Figs. 8–10 show the contour plots of R_0 with respect to β and α, p and δ, κ and q, γ and η in three stages. It indicates that increasing the effective coverage rate of wearing masks α, recovery rate of symptomatic infected individuals γ, the rate of keeping social distance η can stem the transmission of COVID-19 in three stages. Nevertheless, reducing the transmission rate β, progression rate p from $E(t)$ to $A(t)$ and progression rate κ from $A(t)$ to $I(t)$ also can control

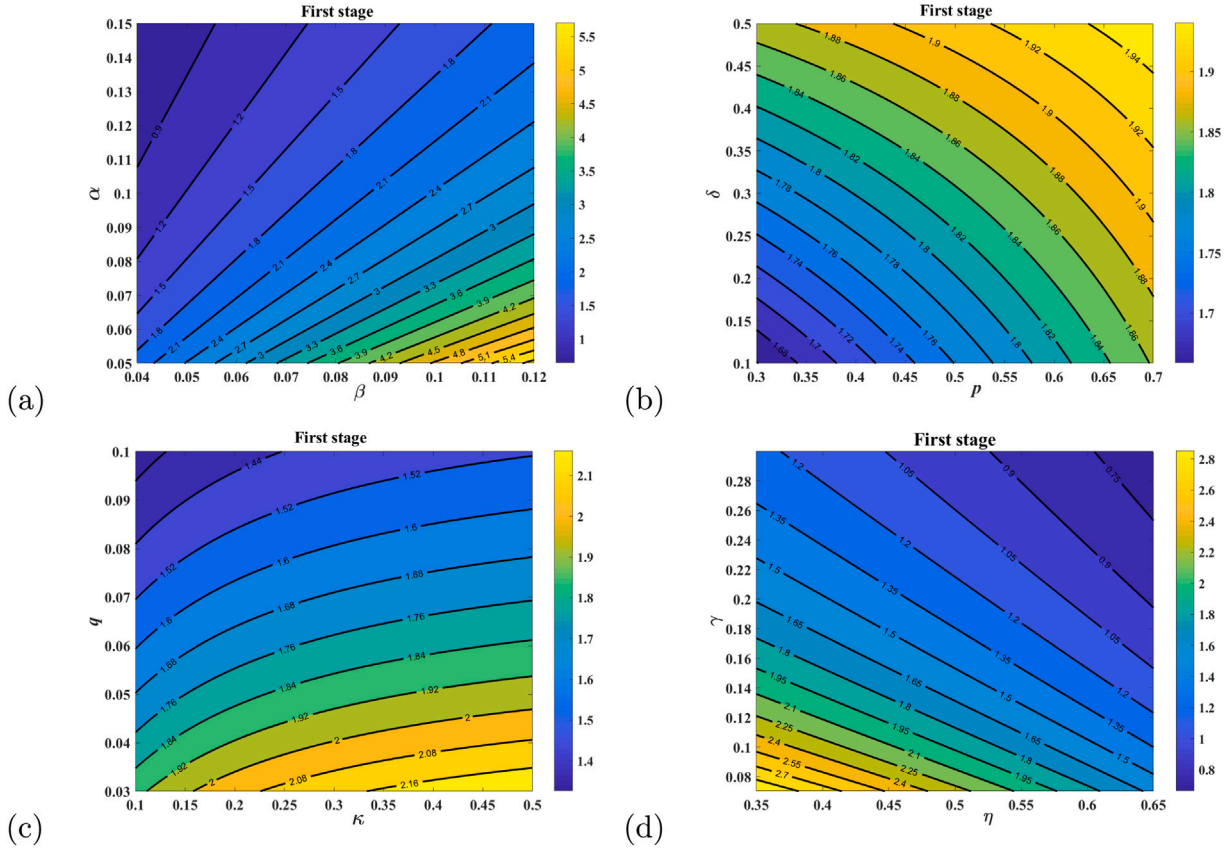

Fig. 8. Contour plot of R_0 in the first stage. (a) Contour plot of R_0 varies β and α. (b) Contour plot of R_0 varies δ and p. (c) Contour plot of R_0 varies q and κ. (d) Contour plot of R_0 varies η and γ.

the spread of COVID-19 in all the stages. In addition, we discover that enlarging the proportion of mask use is more effective than increasing the proportion of keeping social distance in controlling the transmission of COVID-19 in New York City. It still provides new insights into preventing the spread of COVID-19 in the real world.

The impact of mask use on the spread of COVID-19

Herein, our focus is to investigate the impact of masks on the spread of COVID-19 in this segment. Furthermore, we illustrated the variation of R_0 with respect to the effective coverage of using face masks α and observed that R_0 decreases rapidly with increase the value of α and α exceed a certain value $\alpha_c = 0.182$, R_0 becomes smaller than 1 from Fig. 11(a). Thus, increasing the coverage of mask use at the beginning spread of the disease is more effective in controlling the disease. We can obtain the mean value of the basic reproduction number in the first stage of NYC is $R_0 = 1.822$, which means the first stage is very serious in NYC, although confirmed cases are rare. The epidemic would rapidly break out if no intervention was taken. From Fig. 11(b) we can conclude if the effective coverage rate of mask use increased to $\alpha = 0.2$ before the US Centers for CDC recommending public wear masks, the number of confirmed cases will fall by 25,000 up to 03 April, 2020. It can be seen that the greater coverage rate of mask use in NYC, cumulative confirmed cases will be decreased quickly and the smaller final scale form Fig. 11 (c,d). If public keep the effective rate of wearing masks at 0.14 in the second, the cumulative number of cases will increase 4 times and reach 1.05 million up to 07 June, 2020. We can obtain the mean value of the basic reproduction number in the second stage of NYC is $R_0 = 0.6483$. If the effective coverage of mask use in public reaches 50% at the early stage of disease transmission, cumulative confirmed cases will be reduced from 71,178 to about 35,000 up to 03 April, 2020. If mask coverage stays at this level in the second, the cumulative confirmed cases will be cut off 30% in the second stage, and reduced from 0.201 million to 0.145 million up to 07 June, 2020 from Fig. 11(c). However, when the effective coverage rate of masks reaches a certain level $\alpha = 0.5$, increasing the value of α, the benefits are not obvious compared to the cost of wasting scale medical resources. This means that other control measures are needed to contain the disease. If the effective rate of mask use is reduced to 0.2 after reopening, the number of cumulative infected cases will expand 8 times and break through 2 million on 31 October, 2020 from Fig. 11(d). Based on the fitting result, we can roughly calculate the effective reproduction number $R_0 = 1.024$ in the third stage. From the epidemiological point of view, the disease will break out in the long run. Therefore, multiple control measures are needed to stem the spread of COVID-19 in New York City.

Theory of validation

Finally, we will illustrate our theoretical results of model (1) by numerical simulations. Most of the parameter values for those simulations are selected based on above simulations and each of the equilibria are simulated, respectively. If we take $\alpha = 0.281$, $\beta = 0.075$, $k = 0.361$, other parameter values are the same as the values in Table 2, then we obtain $R_0 = 0.6483 < 1$. We can derive that disease-free equilibrium $P^*(13363028, 0, 0, 0, 0)$ is globally asymptotically stable from Theorem 1. The simulation results in Fig. 12(a) demonstrate that the exposed, asymptomatic, symptomatic, quarantined in the hospital

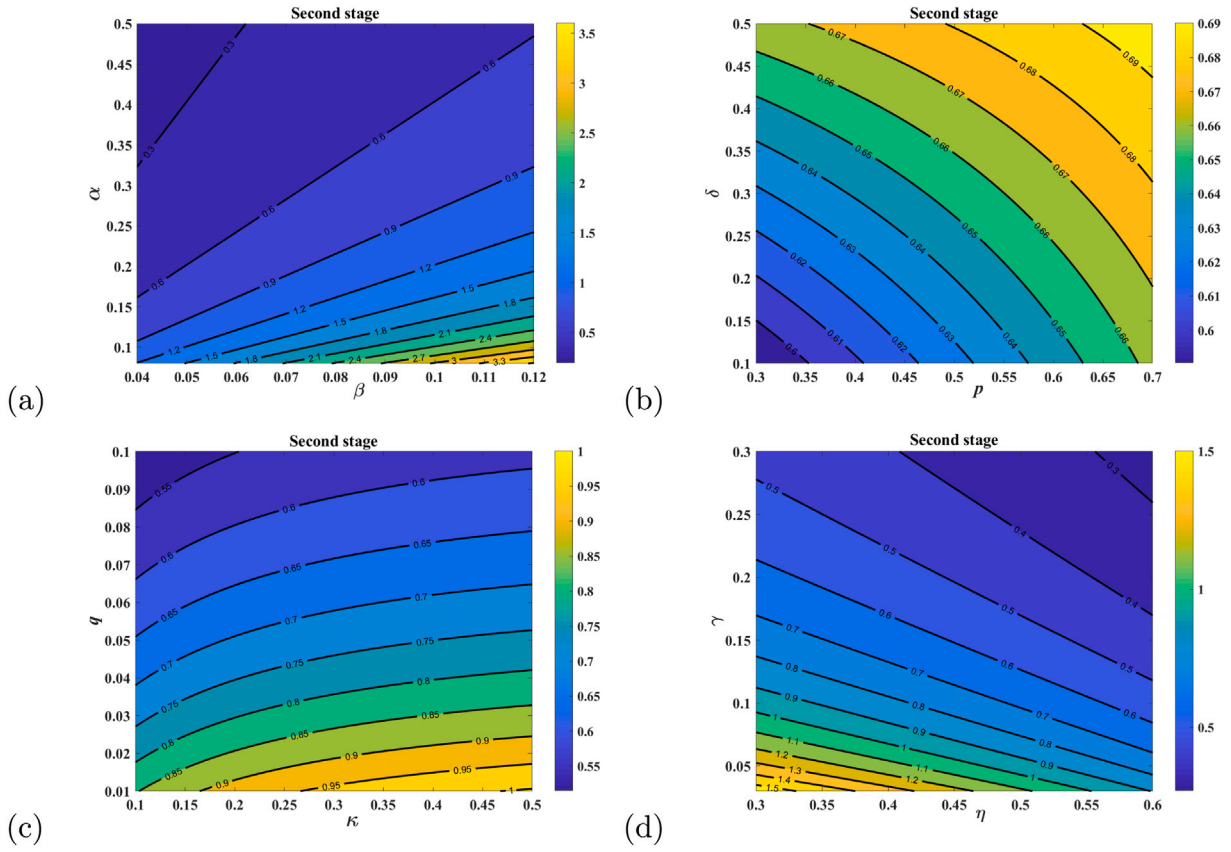

Fig. 9. Contour plot of R_0 in the second stage. (a) Contour plot of R_0 varies β and α. (b) Contour plot of R_0 varies δ and p. (c) Contour plot of R_0 varies q and κ. (d) Contour plot of R_0 varies η and γ.

and removed individuals all die out. When $\alpha = 0.01$, $\beta = 0.045$, and the other parameters values are the same as above simulation, then $R_0 = 1.093$. We can conclude that the endemic equilibrium point $P^*(107, 1560, 298, 1383, 1452, 13\,358\,000)$ of model (1) is globally asymptotically stable from Theorem 3, and we observe that they all maintain the endemic level from Fig. 12(b).

Discussion and conclusion

An SEAIQR epidemic model about COVID-19 transmission is formulated in this work. The basic reproduction number, R_0, of the model is defined and the explicit formula is given upon. A threshold result is obtained: the infectious disease will die out if $R_0 < 1$, and the endemic equilibrium point of the model is globally asymptotically stable if $R_0 > 1$.

Since the accumulative confirmed cases of COVID-19 are rising day by day, the prediction of infected cases is of significant importance for health care arrangements. Since the protective effect of wearing masks on the disease has been controversial in USA, few people in the public wear masks in the liberal and democratic society of the US. There are some experimental researches suggest that mask use may be useful intervention strategy in controlling respiratory infectious disease under coughing conditions [11–13]. Cui eta [38] adopted a SEIR model to investigate the intervention strategy he influence of wearing N95 face masks in reducing the spread of influenza H1N1, and conclude that mask use is an effective method in controlling the transmission of influenza H1N1. Steffen E et al. [7] develop a compartmental model to assess the impact of mask use by the general and the potential high value of public use of masks in reducing the transmission and the burden of the pandemic.

In this work, we devised an SEAIQR model to investigate the impact of coverage rate of mask use on the COVID-19 transmission, and fit the accumulative confirmed cases of COVID-19 in New York City. The crucial model parameters have been estimated by the Latin Hypercube Sampling and the MCMC method. We also made the sensitivity analysis of the key parameters, and obtained that the transmission rate β, the coverage rate of mask use α and the effectiveness of keeping social distance η have significant effect on the basic reproduction number R_0 from the PRCC values of parameters. From the variation of R_0 with respect to the effective coverage of mask use α, we can observe that α exceed a certain value $\alpha_c = 0.182$, R_0 becomes smaller than 1 in the second stage. Based on mathematical analysis and data fitting, we obtain the mean value of effective basic reproduction number of the first stage from March 20 to April 03 2020 in NYC is $R_0 = 1.822$. Wilder et al. obtain that the basic reproduction number R_0 in the New York City is 3.2 (95% CI: 2.71 to 3.93) [19]. Zou et al. revealed that the basic reproduction number R_0 in the US and New York state are 2.5 and 3.6 respectively [39] and Peirlinck et al. 5.3 (95% CI: 4.35 to 6.25) in the New York City [40]. Gunzler et al. concluded that the basic reproduction numbers R_0 in the New York City are 4.3 (95% CI: 4.2 to 4.4) on March 17, 1.39 (95% CI: 1.36 to 1.42) on March 24 and 1.21 (95% CI: 1.17 to 1.26) on April 01, respectively [41]. Our results about the value of R_0 keep consistent with research [17,19,41], the effective reproduction number is closely related to time. We obtain that the greater coverage rate of mask use in New York City, cumulative confirmed cases will be decreased quickly. However, when the effective coverage of masks reaches a certain level $\alpha = 0.6$, increase the effective coverage rate α, the benefits are not obvious compared to the cost of wasting scale medical resources. If the effective coverage of mask use

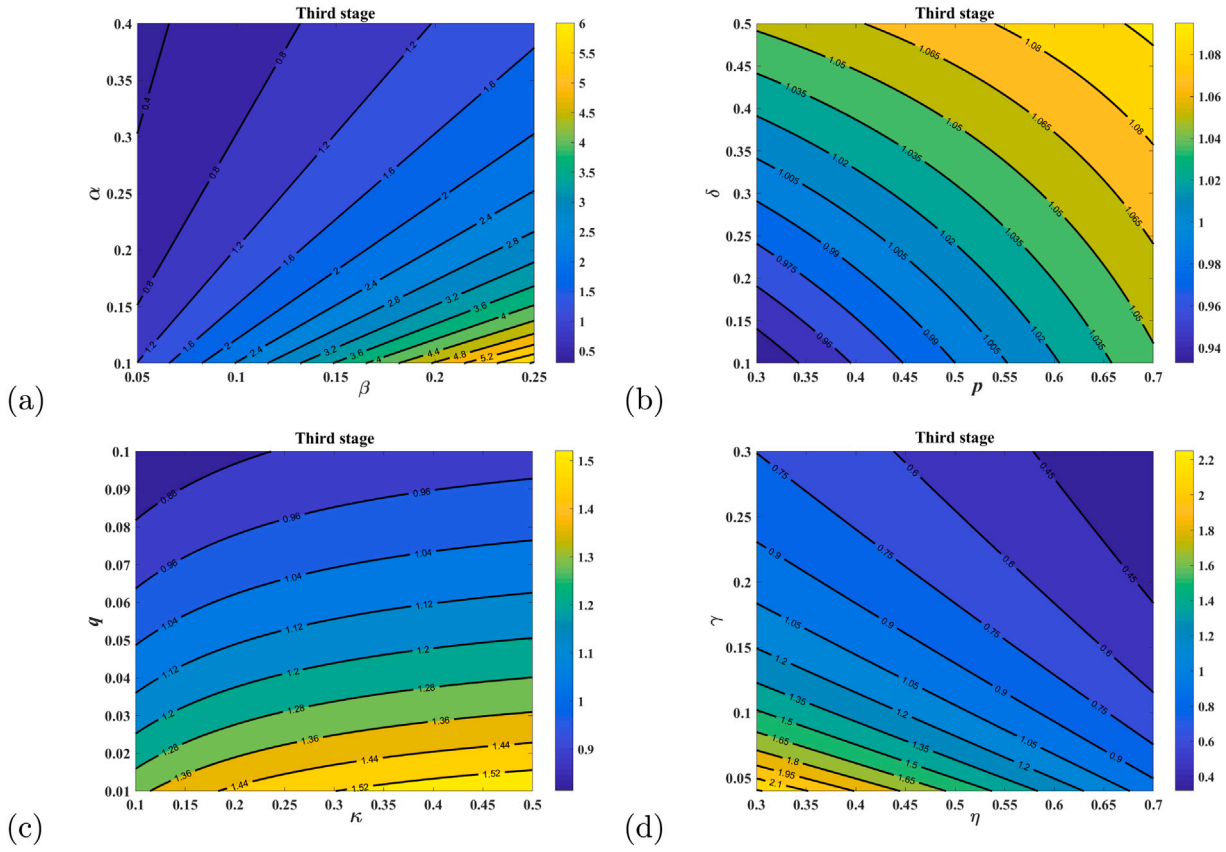

Fig. 10. Contour plot of R_0 in the third stage. (a) Contour plot of R_0 varies β and α. (b) Contour plot of R_0 varies δ and p. (c) Contour plot of R_0 varies q and κ. (d) Contour plot of R_0 varies η and γ.

in public reaches 0.5 in the first stage, cumulative confirmed cases will be reduced about 50% and the outbreak will eventually be contained under existing control measures in long time. Hundreds of thousands of infected people could be decreased if masks were more widely used in the early stages and the epidemic will be less severe. Here, parameter α is equal to the coverage rate of mask use products the efficacy of mask. The efficacy of mask use to prevent infection is about 66%–93% based on a research about the effectiveness of mask use for COVID-19 [42]. If we suppose efficacy of mask use is 70%, we can obtain only the coverage rate reaches to 85.7% can α reaches 60%. In practice, it is hard to reach the rate of people wearing masks. Shen estimated the proportion of people who always wear a face mask in New York is 76.6% based on about 250,000 interviews conducted by Dynata from 02 July to 14 July, 2020 from The New York Times [8,43]. Moreover, the coverage rate of wearing mask is varying over time. The coverage rate of mask use by the public is very low in the early stage of the epidemic. As the epidemic became more severe, the WHO suggested the public wearing masks, people began to wear masks gradually. The parameter critical value α_c we estimate is an average value from 04 April to 07 June. Therefore, it is very difficult to eliminate the epidemic in New York City in a short time.

With the relieving of lockdown in New York City, people began to go back to work on June 8 [8]. Under these circumstances, the contacts between people are relatively frequent, and thus it will increase the risk of transmission. In this case, COVID-19 continued to spread in New York City. To control the epidemic, it is still necessary to decrease the contact number, increase the coverage rate of masks use and take personal protection in public places. To achieve this goal, people should make rather less contacts with infected individuals, keep social distance and minimize unnecessary outings. Infected cases should be diagnosed and treated in hospital as soon as possible to ensure that infected individuals do not spread the disease further, increase the coverage rate of mask use and take personal protection in public places. Meanwhile, the immunization is also necessary. These strategies, if successful, would control the COVID-19 in New York city in the near future. Meanwhile, spatial effects should be included in the dynamical models from theoretical perspective of view [44–46].

Declaration of competing interest

The authors declare that they have no known competing financial interests or personal relationships that could have appeared to influence the work reported in this paper.

Acknowledgments

The authors would like to thank the anonymous reviewer for their valuable suggestions and their useful comments that contributed to improve this manuscript.

This work is supported by National Natural Science Foundation of China under Grant Nos. 12022113, 12126416 and 12101573, Henry Fok foundation for young teachers (171002), Program for the Outstanding Innovative Teams (OIT) of Higher Learning Institutions of Shanxi, Outstanding Young Talents Support Plan of Shanxi province, and Natural Science Foundation of Shanxi Province Grant No. 201801D221003, Graduate Innovation Project of Shanxi Province (2021Y625).

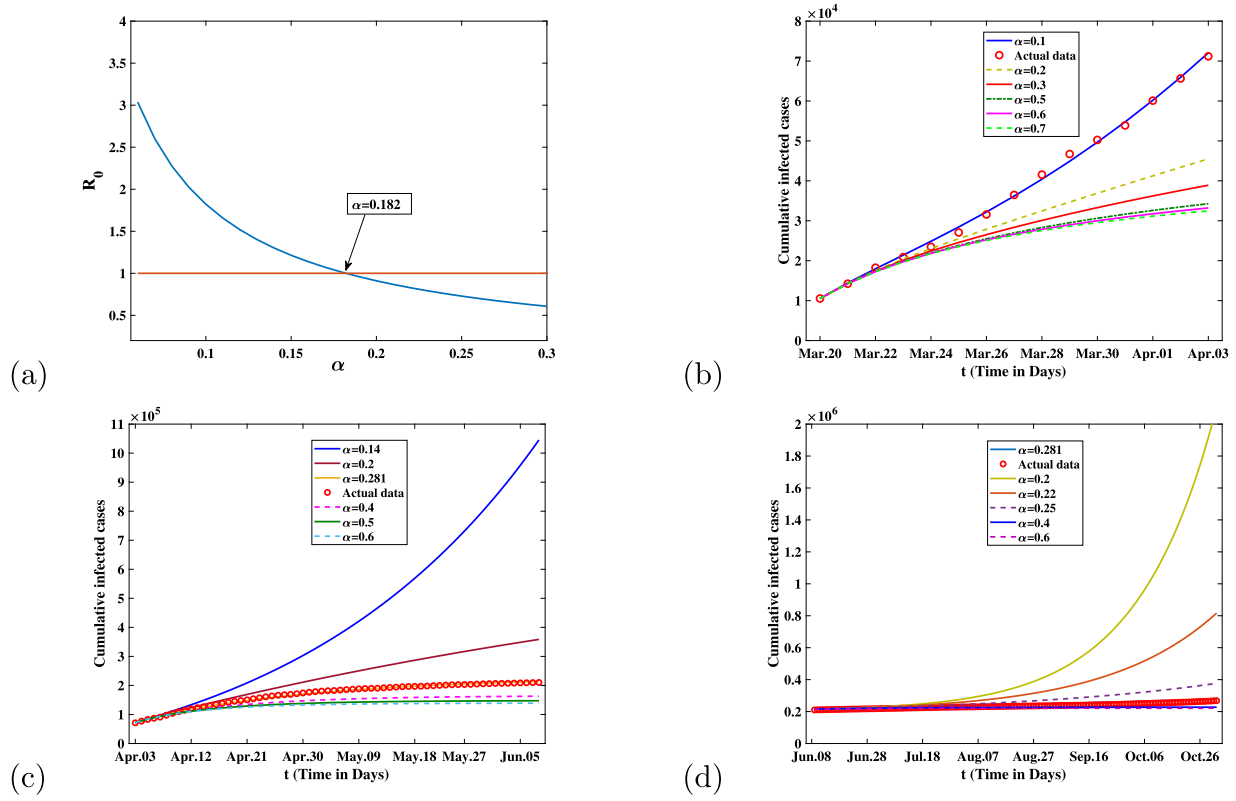

Fig. 11. (a) The variation of R_0 with respect to the coverage of mask use α; (b) Confirmed cases with different α in New York City of the first stage; (c) Confirmed cases with different α in New York City of the second stage; (d) Confirmed cases with different α in New York City of the third stage. The red circles are the number of cumulative infected cases.

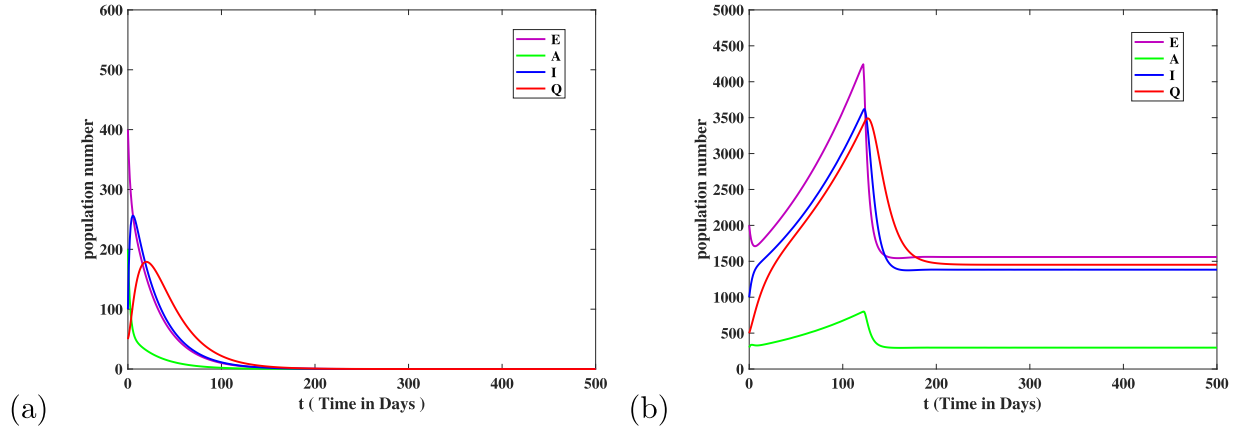

Fig. 12. (a) The global stability of equilibrium P^0 with $R_0 = 0.6483$; (b) the global stability of equilibrium P^* with $R_0 = 1.093$.

References

[1] Chen Y, Liu Q, Guo D. Emerging coronaviruses: Genome structure, replication, and pathogenesis. J Med Virol 2020;92:1–6.

[2] Gralinski LE, Menachery VD. Return of the coronavirus: 2019-nCoV. Viruses 2020;12:135–42.

[3] World Health Organization. 2020, https://www.who.int/health-topics/coronavirus. Accessed on 8 october 2020.

[4] Zhou W, Wang A, Xia F, et al. Effects of media reporting on mitigating spread of COVID-19 in the early phase of the outbreak. Math Biosci Eng 2020;17:2693–707.

[5] Tian H, Chen B, Li Y, et al. An investigation of transmission control measures during the first 50 days of the COVID-19 epidemic in China. Science 2020;368:638–42.

[6] Center for Systems Science and Engineering at Johns Hopkins University. COVID-19. Github repository; 2020, https://github.com/CSSEGISandData/COVID-19. Accessed 2 October 2020.

[7] Eikenberry SE, Mancuso M, Iboi E, et al. To mask or not to mask: Modeling the potential for face mask use by the general public to curtail the COVID-19 pandemic. Infect Dis Mod 2020;5:293–308.

[8] The New York times and Dynata. Mask-wearing survey data. New York Times; 2020, https://github.com/nytimes/covid-19-data/blob/master/mask-use/mask-use-bycounty.csv.

[9] https://covidmapper.ca/geomap/. Accessed on 31 october 2020.

[10] Macintyre CR, Chughtai AA, Rahman B, et al. The efficacy of medical masks and respirators against respiratory infection in healthcare workers. Influ Other Respir Viruses 2017;11:511–7.

[11] Tracht SM, Del VS, Hyman JM, et al. Mathematical modeling of the effectiveness of facemasks in reducing the spread of novel influenza A (H1N1). PLoS One 2010;5:e9018.

[12] Hung CK, Kwok-Yung Y. COVID-19 epidemic: disentangling the re-emerging controversy about medical facemasks from an epidemiological perspective. Int J Epidemiol 2020;49:1063–6.

[13] Li R, Pei S, Chen B, et al. Substantial undocumented infection facilitates the rapid dissemination of novel coronavirus (SARS-CoV2). Science 2020;368:489–93.

[14] Jason WC, Ng CY, Brook RH. Response to COVID-19 in taiwan: Big data analytics, new technology, and proactive testing. JAMA 2020;323:1341–2.
[15] Wu J, Xu FJ, Zhou WD, et al. Risk factors for SARS among persons without known contact with SARS patients, Beijing, China. Emerg Infect Dis 2004;10:210–6.
[16] Lau JT, Tsui H, Lau M, et al. SARS transmission, risk factors, and prevention in Hong Kong. Emerg Infect Dis 2004;10:587–92.
[17] Harrichandra A, Ierardi AM, Pavilonis B. An estimation of airborne SARS-CoV-2 infection transmission risk in New York City nail salons. Toxicol Ind Health 2020. http://dx.doi.org/10.1177/0748233720964650.
[18] Alagoz O, Ajay KS, Brian WP, et al. Effect of timing of and adherence to social distancing measures on COVID-19 burden in the United States. Ann Intern Med 2020. http://dx.doi.org/10.7326/M20-4096.
[19] Wilder B, Charpignon M, Killian JA, et al. Modeling between-population variation in COVID-19 dynamics in Hubei, Lombardy, and New York City. Proc Natl Acad Sci 2020;41:25904–10.
[20] Tang B, Bragazzi NL, Li Q, et al. An updated estimation of the risk of transmission of the novel coronavirus (2019-nCov). Infect Dis Mod 2020;5:248–55.
[21] Sun GQ, Wang SF, Li MT, et al. Transmission dynamics of COVID-19 in Wuhan, China: effects of lockdown and medical resources. Nonlinear Dynam 2020;101:1981–93.
[22] Diekmann O, Heesterbeek JA, Metz AJ. On the definition and the computation of the basic reproduction ratio R_0 in models for infectious diseases. J Math Biol 1990;28:365–82.
[23] Dreessche P, Watmough J. Reproduction numbers and sub-threshold endemic equilibria for compartmental models of disease transmission. Math Biosci 2002;180:29–48.
[24] Atangana A. Mathematical model of survival of fractional calculus, critics and their impact: How singular is our world? Adv Differential Equations 2021;1:2021.
[25] Martcheva M. An introduction to mathematical epidemiology. New York: Springer; 2015.
[26] LaSalle JP. Ser. regional conference series in applied mathematics. In: The stability of dynamical systems. Philadelphia, PA, USA: SIAM; 1976, p. 1096–105.
[27] Salceanu P, Smith H. Persistence in a discrete-time, stage-structured epidemic model. J Differ Equ Appl 2001;16:73–103.
[28] Zhao XQ. Dynamical systems in population biology. New York: Springer-Verlag; 2003.
[29] Business Insider. US CDC asks states to prepare for distribution of potential COVID-19 vaccine by November 1. 2020, Published online 2020. https://www.businessinsider.in/science/health/news/us-cdc-asks-states-to-prepare-for-distribution-of-potential-covid-19-vaccine-by-november-1/articleshow/77905321.cms.
[30] Robert Wood Johnson Foundation University of Wisconsin Population Health Institute. County health rankings & roadmaps. 2020, http://www.countyhealthrankings.org. Accessed July 5, 2020.
[31] Ferguson N, Laydon D, Nedjati GG, et al. Report 9: Impact of non-pharmaceutical interventions (NPIs) to reduce COVID19 mortality and healthcare demand. Medrxiv http://dx.doi.org/10.25561/77482.
[32] Li Q, Guan XH, Wu P, et al. Early transmission dynamics in Wuhan, China, of novel coronavirus-infected pneumonia. N Engl J Med 2020;382:1199–207.
[33] Zhou F, Yu R, Du H, et al. Clinical course and risk factors for mortality of adult inpatients with COVID-19 in Wuhan, China: a retrospective cohort study. Lancet 2020;395:1054–62.
[34] https://covid19.healthdata.org/united-states-of-america?view=mask-use&tab=trend. Accessed on 5 october 2020.
[35] Haario H, Laine M, Mira A, et al. DRAM: Efficient adaptive MCMC. Stat Comput 2006;16:339–54.
[36] Gamerman D, Lopes HF. Markov Chain Monto Carlo: Stochastic simulation for bayesian inference. 2nd ed.. London, New York: Taylor and Francis Group; 2006.
[37] Marino S, Hogue IB, Ray JC, et al. A methodology for performing global uncertainty and sensitivity analysis in systems biology. J Theoret Biol 2008;254:178–96.
[38] Cui JA, Zhang YN, Feng ZL, et al. Influence of asymptomatic infections for the effectiveness of facemasks during pandemic influenza. Math Biosci Eng 2019;16:3936–46.
[39] Zou DF, Wang LX, Xu P, et al. Epidemic model guided machine learning for COVID-19 forecasts in the United States. Medrxiv http://dx.doi.org/10.1101/2020.05.24.20111989.
[40] Peirlinck M, Linka K, Costabal FS, et al. Outbreak dynamics of COVID-19 in China and the United States. Biomech Model Mech 2020;19:2179–93.
[41] Gunzler D, Sehgal AR. Time-varying COVID-19 reproduction number in the United States. Medrxiv http://dx.doi.org/10.1101/2020.04.10.20060863.
[42] Chu DK, Akl EA, Duda S, et al. Physical distancing, face masks, and eye protection to prevent person-to-person transmission of SARS-CoV-2 and COVID-19: a systematic review and meta-analysis. Lancet 2020. Published online 2020.
[43] Shen MW, Zu J, Christopher K, et al. Projected COVID-19 epidemic in the United States in the context of the effectiveness of a potential vaccine and implications for social distancing and face mask use. Vaccine 2021;39:2295–302.
[44] Guo ZG, Sun GQ, Wang Z, Jin Z, Li L, Li C. Spatial dynamics of an epidemic model with nonlocal infection. Appl Math Comput 2020;377:125158.
[45] Sun GQ, Jusup M, Jin Z, Wang Y, Wang Z. Pattern transitions in spatial epidemics: mechanisms and emergent properties. Phys Life Rev 2016;19:43–73.
[46] Jia JS, Lu X, Yuan Y, Xu G, Jia J, Christakis NA. Population flow drives spatio-temporal distribution of COVID-19 in China. Nature 2020;582:389–94.